

# Quantifying the Redshift Space Distortion of the Bispectrum II: Induced Non-Gaussianity at Second Order Perturbation

Arindam Mazumdar<sup>1\*</sup>, Somnath Bharadwaj<sup>1,2†</sup>, Debanjan Sarkar<sup>1,3‡</sup>

<sup>1</sup>Centre for Theoretical Studies, Indian Institute of Technology Kharagpur, Kharagpur - 721302, India

<sup>2</sup>Department of Physics, Indian Institute of Technology Kharagpur, Kharagpur - 721302, India

<sup>3</sup>Department of Physics, Ben-Gurion University of the Negev, Be'er Sheva - 84105, Israel

## ABSTRACT

The anisotropy of the redshift space bispectrum  $B^s(\mathbf{k}_1, \mathbf{k}_2, \mathbf{k}_3)$ , which contains a wealth of cosmological information, is completely quantified using multipole moments  $\bar{B}_\ell^m(k_1, \mu, t)$  where  $k_1$ , the length of the largest side, and  $(\mu, t)$  respectively quantify the size and shape of the triangle  $(\mathbf{k}_1, \mathbf{k}_2, \mathbf{k}_3)$ . We present analytical expressions for all the multipoles which are predicted to be non-zero ( $\ell \leq 8, m \leq 6$ ) at second order perturbation theory. The multipoles also depend on  $\beta_1, b_1$  and  $\gamma_2$ , which quantify the linear redshift distortion parameter, linear bias and quadratic bias respectively. Considering triangles of all possible shapes, we analyse the shape dependence of all of the multipoles holding  $k_1 = 0.2 \text{ Mpc}^{-1}, \beta_1 = 1, b_1 = 1$  and  $\gamma_2 = 0$  fixed. The monopole  $\bar{B}_0^0$ , which is positive everywhere, is minimum for equilateral triangles.  $\bar{B}_0^0$  increases towards linear triangles, and is maximum for linear triangles close to the squeezed limit. Both  $\bar{B}_2^0$  and  $\bar{B}_4^0$  are similar to  $\bar{B}_0^0$ , however the quadrupole  $\bar{B}_2^0$  exceeds  $\bar{B}_0^0$  over a significant range of shapes. The other multipoles, many of which become negative, have magnitudes smaller than  $\bar{B}_0^0$ . In most cases the maxima or minima, or both, occur very close to the squeezed limit.  $|\bar{B}_\ell^m|$  is found to decrease rapidly if  $\ell$  or  $m$  are increased. The shape dependence shown here is characteristic of non-linear gravitational clustering. Non-linear bias, if present, will lead to a different shape dependence.

**Key words:** methods: statistical – cosmology: theory – large-scale structures of Universe.

## 1 INTRODUCTION

The simplest models of inflation predict the primordial density fluctuations which seed the large-scale structures in the Universe to be a Gaussian random field (Baumann 2009), Cosmic Microwave Background (CMB) measurements (Fergusson et al. 2012; Oppizzi et al. 2018; Planck Collaboration et al. 2019; Shiraishi 2019) and galaxy surveys (Feldman et al. 2001; Scoccimarro et al. 2004; Liguori et al. 2010; Ballardini et al. 2019) have been used to place tight constraints on primordial non-Gaussianity. These density fluctuations are however predicted to become non-Gaussian as they evolve (induced non-Gaussianity; Fry 1984) due to the non-linear growth and non-linear biasing. It is therefore necessary to consider higher order statistics, the three-point correlation function or its Fourier conjugate the bispectrum

being the lowest order statistic sensitive to non-Gaussianity. Second order perturbation theory predicts (Matarrese et al. 1997) that measurements of the bispectrum in the weakly non-linear regime can be used to determine the bias parameters, and this has been employed in the galaxy surveys to quantify the galaxy bias parameters (Feldman et al. 2001; Scoccimarro et al. 2001; Verde et al. 2002; Nishimichi et al. 2007; Gil-Marín et al. 2015). Further, the measurements of bispectrum enable us to lift the degeneracy between  $\Omega_m$  (which appears in  $f(\Omega_m)$ ) and  $b_1$ , something which is not possible by considering only the power spectrum (Scoccimarro et al. 1999a).

Redshift space distortion (RSD) is a prominent feature in redshift surveys which probe the large scale structures observed in the Universe. At small length-scales random motions make the structures appear elongated along line of sight (LoS) leading to the well known Finger of God (FoG) effect (Jackson 1972). At large length-scales RSD causes the over-dense regions to appear more over-dense and the under-dense regions to appear more under-dense

\* arindam.mazumdar@iitkgp.ac.in

† somnath@phy.iitkgp.ernet.in

‡ debanjan@post.bgu.ac.il

along the LoS (Kaiser 1987). At large length-scales where linear perturbation theory may be assumed to hold, the redshift space power spectrum of a linearly biased tracer,  $P^s(\mathbf{k}_1)$ , is related to the real space power spectrum  $P^r(k_1)$  as  $P^s(\mathbf{k}_1) = (1 + \beta_1 \mu_1^2)^2 P^r(k_1)$  (Kaiser 1987) where  $\beta_1 = f/b_1$  is the linear redshift distortion parameter. Here  $f$  is logarithmic derivative of the growth rate of density perturbation in linear theory and this is a function of cosmological matter density parameter  $\Omega_m$ .  $b_1$  is linear bias factor and  $\mu_1 = \hat{\mathbf{z}} \cdot \mathbf{k}_1/k_1$  where  $\hat{\mathbf{z}}$  points towards the LoS direction. The redshift space power spectrum  $P^s(\mathbf{k}_1)$  is anisotropic *i.e.* it depends on how  $\mathbf{k}_1$  is oriented with respect to  $\hat{\mathbf{z}}$ . This anisotropy can be quantified by expanding  $P^s(\mathbf{k}_1)$  in terms of Legendre polynomials in  $\mu_1$ , the reader is referred to an extensive review (Hamilton 1998) of linear RSD for details. The anisotropy of the redshift space power-spectrum contains a rich wealth of cosmological information. For example, the parameter  $f$  can be estimated (Loveday et al. 1996; Peacock et al. 2001; Hawkins et al. 2003; Guzzo et al. 2008), the total mass of massive neutrinos can be constrained (Hu et al. 1998; Upadhye 2019), and dark energy theories and modified gravity theories can be tested (Linder 2008; Song & Percival 2009; de la Torre et al. 2017; Johnson et al. 2016; Mueller et al. 2018).

In this paper we consider the redshift space bispectrum  $B^s(\mathbf{k}_1, \mathbf{k}_2, \mathbf{k}_3)$  which is induced at second order perturbation theory starting from Gaussian initial conditions. In addition to the size and shape of the triangle  $(\mathbf{k}_1, \mathbf{k}_2, \mathbf{k}_3)$ , the redshift space bispectrum also depends on how the three vectors are oriented with respect to  $\hat{\mathbf{z}}$ . Like the power spectrum, the anisotropy of  $B^s(\mathbf{k}_1, \mathbf{k}_2, \mathbf{k}_3)$  contains a wealth of cosmological information, and it is important to accurately model and quantify this. Hivon et al. (1995) and Verde et al. (1998c) have calculated the bispectrum in redshift space. However, the focus in these works has been on measuring the large scale bias and the cosmological parameters, and they have not quantified the RSD anisotropy. Scoccimarro et al. (1999a) have quantified the anisotropy of the redshift space bispectrum by decomposing it into spherical harmonics. However, they have only considered the monopole and one quadrupole component ( $\ell = 2, m = 0$ ). Hashimoto et al. (2017) also have considered a single quadrupole component of the redshift space bispectrum. The works mentioned above are all use non-linear perturbation theory, and their results are extensively validated using large cosmological N-body simulations. However, these works do not carry out a complete analysis of the anisotropy, and are restricted to a single quadrupole component and a very limited set of triangle configurations. Nan et al. (2018) have presented approximate analytical expressions based on the halo model for the higher angular multipole moments up to  $\ell = 4$ , and they have analysed these for a limited set of triangle configurations. Yankelevich & Porciani (2019) and Gualdi & Verde (2020) forecast cosmological parameter constraints including the redshift space bispectrum and power spectrum. Desjacques et al. (2018) have used effective field theory to accurately model the redshift space bispectrum on mildly non-linear scales. Clarkson et al. 2019 and de Weerd et al. (2020) have recently shown that relativistic effects will introduce a dipole anisotropy in the redshift space bispectrum on very large length-scales. Slepian & Eisenstein (2017), Slepian & Eisenstein (2018) present a technique to quantify the red-

shift space three-point correlation function by expanding it in terms of products of two spherical harmonics, whereas Sugiyama et al. (2019) have proposed a tri-polar spherical harmonic decomposition to quantify the anisotropy of the redshift space bispectrum which they demonstrate by applying it to the Baryon Oscillation Spectroscopic Survey (BOSS) Data Release 12. The last two works mentioned here present very efficient computational techniques for quantifying the three point statistics in large galaxy surveys.

In a recent work (Bharadwaj et al. 2020) (hereafter referred to as Paper I) we have proposed a new technique to quantify the anisotropy of the redshift space bispectrum. We have decomposed the redshift space bispectrum in spherical harmonics which completely quantify the anisotropy. We illustrate this by considering the linear RSD of the bispectrum arising from primordial non-Gaussianity. Only the first four even  $\ell$  multipoles (up to  $\ell = 6, m = 4$ ) are found to be non-zero, and we have presented explicit analytical expressions for these. We find that the ratio of the different multipole moments to the real space bispectrum are cubic polynomials in  $\beta_1$  the linear redshift distortion parameter. The coefficients of these polynomials depend only on the shape of the triangle. We have analysed all the non-zero multipole moments for triangles of all possible shapes. If measured in future, the various multipole moments of the bispectrum of primordial non-Gaussianity hold the potential of constraining  $\beta_1$ . The results presented in Paper I are also important to constrain  $f_{\text{NL}}$  using redshift surveys.

In the present paper we have applied the formalism developed in Paper I to quantify the anisotropy of the induced redshift space at second order perturbation theory. We present explicit analytical formulas for all the non-zero multipole moments of the induced redshift space bispectrum. Considering triangles of all possible shapes, we analyse the variation of different multipole moments with the shape of the triangle. A brief outline of the rest of the paper follows. In Section 2 we briefly summarize some of the salient features of the formalism developed in Paper I. We first apply the formalism (Section 3) to quantify and analyse the shape dependence of the real space bispectrum. In Section 4 we develop the methodology and notation to calculate the multipole moments of the induced redshift space bispectrum. The final expression for the  $\ell, m$  multipole refers to three terms namely  $R$  whose multipole moments are presented in Paper I,  $S$  and  $T$  whose multipole moments are presented in Appendix A and B respectively. We present the results in section 5, whereas section 6 presents Summary and Discussion.

We have used the  $\Lambda$ CDM power spectrum generated by the Blotzmann code CLASS (Lesgourgues 2011; Blas et al. 2011) with the cosmological parameters fixed from Planck 2015 results Planck Collaboration et al. 2016.

## 2 FORMALISM

The bispectrum is defined as

$$B(\mathbf{k}_1, \mathbf{k}_2, \mathbf{k}_3) = V^{-1} \langle \Delta(\mathbf{k}_1) \Delta(\mathbf{k}_2) \Delta(\mathbf{k}_3) \rangle, \quad (1)$$

where the  $\Delta(\mathbf{k})$ s refer to the Fourier components of the density contrast. The three vectors involved in the bispectrum are constrained to form a closed triangle, *i.e.*  $\mathbf{k}_1 + \mathbf{k}_2 + \mathbf{k}_3 = 0$

(Figure 1). We label the three sides of the triangle such that  $k_1 \geq k_2 \geq k_3$  where  $k_1 = |\mathbf{k}_1|$ , etc. The real space bispectrum  $B^r(\mathbf{k}_1, \mathbf{k}_2, \mathbf{k}_3)$  is independent of how the triangle is oriented in space, and it depends only on the size and shape of the triangle. Following Paper I, we use the length of the largest side  $k_1$  to parameterize the size of the triangle, and we parameterize the shape using  $\mu = \cos \theta = -\mathbf{k}_1 \cdot \mathbf{k}_2 / (k_1 k_2)$  which is the cosine of the angle between  $-\mathbf{k}_2$  and  $\mathbf{k}_1$ , and  $t = k_2/k_1$  which is the ratio of the second largest side to the largest side. The values of  $\mu$  and  $t$  are restricted to the range

$$0.5 \leq t, \mu \leq 1 \text{ and } 2\mu t \geq 1, \quad (2)$$

and these uniquely specify the shapes of all possible triangles. Figure 2 of Paper I provides a detailed description of the triangle shape corresponding to different values of the parameters  $(\mu, t)$ . For completeness, we summarize this later in this paper when we analyze the shape dependence of the real space bispectrum. In the subsequent discussion we use  $B^r(k_1, \mu, t)$  to parameterize the shape and size dependence of the real space bispectrum. Further, it is convenient to use the notation  $s = k_3/k_1 = \sqrt{t^2 - 2\mu t + 1}$ .

The redshift space bispectrum  $B^s(\mathbf{k}_1, \mathbf{k}_2, \mathbf{k}_3)$ , unlike its real space counterpart, depends on the orientations of the triangles with respect to the line of sight (LoS) direction  $\hat{\mathbf{z}}$ . This anisotropy or orientation dependence arises through  $\mu_1, \mu_2, \mu_3$  which are respectively the cosine of the angles between  $\mathbf{k}_1, \mathbf{k}_2, \mathbf{k}_3$  and  $\hat{\mathbf{z}}$ . It is necessary to consider a triangle with a fixed size and shape, and vary its orientation in order to quantify the anisotropy arising from RSD. As discussed in Paper I, this can be achieved by applying rigid body rotations to a triangle whose size and shape are fixed. It is then possible to parameterize the redshift space bispectrum as  $B^s(\alpha, \beta, \gamma, k_1, \mu, t)$  where  $(\alpha, \beta, \gamma)$  are three angles needed to parameterize the rigid body rotations. However, for the analytical estimates presented in Paper I and continued in this paper, it suffices to parameterize the redshift space bispectrum as  $B^s(\hat{\mathbf{p}}, k_1, \mu, t)$  where  $\hat{\mathbf{p}}$  is a unit vector which can vary over all possible directions. We have

$$\begin{aligned} \mu_1 &= p_z \\ \mu_2 &= -\mu p_z + \sqrt{1 - \mu^2} p_x \\ \mu_3 &= -s^{-1}[(1 - t\mu)p_z + t\sqrt{1 - \mu^2} p_x] \end{aligned} \quad (3)$$

where  $s$  is a function of  $(\mu, t)$  introduced earlier.

We quantify the anisotropy of the redshift space bispectrum  $B^s(\hat{\mathbf{p}}, k_1, \mu, t)$  using the different multipole moments defined as

$$\bar{B}_\ell^m(k_1, \mu, t) = \sqrt{\frac{(2\ell + 1)}{4\pi}} \int [Y_\ell^m(\hat{\mathbf{p}})]^* B^s(\hat{\mathbf{p}}, k_1, \mu, t) d\Omega_{\hat{\mathbf{p}}} \quad (4)$$

where  $Y_\ell^m(\hat{\mathbf{p}})$  are the spherical harmonics and the  $d\Omega_{\hat{\mathbf{p}}}$  integral is over all possible directions of  $\hat{\mathbf{p}}$  which subtends  $4\pi$  steradians. The reader is referred to Paper I regarding the choice of normalization and other details for eq. (4).

The odd multipoles ( $\ell = 1, 3, 5, \dots$ ) are all zero in the plane parallel approximation. We further have  $\bar{B}_\ell^{-m}(k_1, \mu, t) = (-1)^m \bar{B}_\ell^m(k_1, \mu, t)$ , and  $\bar{B}_\ell^m(k_1, \mu, t)$  are all real. Considering linear triangles ( $\mu = 1$ ), the anisotropy is completely quantified by the  $m = 0$  multipole moment and

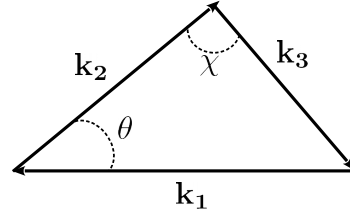


**Figure 1.** This shows a triangle  $(\mathbf{k}_1, \mathbf{k}_2, \mathbf{k}_3)$  which is used to define various parameters used here.

the multipole moments with  $m \neq 0$  are all zero. We however need both the  $m = 0$  and  $m \neq 0$  multipole moments to completely quantify the anisotropy of  $B^s(\hat{\mathbf{p}}, k_1, \mu, t)$  when the three vectors  $\mathbf{k}_1, \mathbf{k}_2$  and  $\mathbf{k}_3$  are not aligned *i.e.* ( $\mu < 1$ ).

### 3 INDUCED REAL SPACE BISPECTRUM

Considering Gaussian initial conditions, non-Gaussianity arises due to the non-linear evolution of the density perturbations (Fry 1984). The bispectrum of induced non-Gaussianity at second order perturbation theory (Scoccimarro et al. 1998a) is given by

$$B^r(\mathbf{k}_1, \mathbf{k}_2, \mathbf{k}_3) = 2b_1^{-1} \left[ F_2(\mathbf{k}_1, \mathbf{k}_2) + \frac{\gamma_2}{2} \right] P^r(k_1) P^r(k_2) + \text{cyc...} \quad (5)$$

where  $b_1$  is the linear bias,  $\gamma_2 = b_2/b_1$  parameterizes the quadratic bias  $b_2$  in terms of  $b_1$ ,  $P^r(k)$  is the real space power spectrum of the tracer for which the bispectrum is being calculated. Here  $P^r(k) = b_1^2 P_m(k)$  where  $P_m(k)$  is the matter power spectrum, and

$$F_2(\mathbf{k}_1, \mathbf{k}_2) = \frac{5}{7} + \frac{\mathbf{k}_1 \cdot \mathbf{k}_2}{2} \left( \frac{1}{k_1^2} + \frac{1}{k_2^2} \right) + \frac{2(\mathbf{k}_1 \cdot \mathbf{k}_2)^2}{7 k_1^2 k_2^2} \quad (6)$$

are the kernels appearing in the second order perturbation for the density contrast (Goroff et al. 1986). The various terms  $F_2(\mathbf{k}_1, \mathbf{k}_2), F_2(\mathbf{k}_2, \mathbf{k}_3), F_2(\mathbf{k}_3, \mathbf{k}_1)$  are dimensionless functions which depend on the shape of the triangle  $(\mathbf{k}_1, \mathbf{k}_2, \mathbf{k}_3)$ , and these have very simple algebraic expressions in terms of  $(\mu, t)$ . Using the compact notation  $F_{12}(\mu, t) = F_2(\mathbf{k}_1, \mathbf{k}_2)$ , etc. we can express these as

$$\begin{aligned} F_{12}(\mu, t) &= \frac{1}{14} \left( 4\mu^2 - 7\mu t - \frac{7\mu}{t} + 10 \right), \\ F_{23}(\mu, t) &= \frac{7\mu + (3 - 10\mu^2)t}{14ts^2}, \\ F_{31}(\mu, t) &= \frac{t^2(-10\mu^2 + 7\mu t + 3)}{14s^2}. \end{aligned} \quad (7)$$

Considering  $b_1$  and  $\gamma_2$  as independent parameters in eq. (5), we see that changing  $b_1$  scales the bispectrum irrespective of the shape and size of the triangle. In contrast,  $\gamma_2$  occurs in combination with  $F_{12}(\mu, t)$ , etc. whose values depend on the shape of the triangle. It has been proposed (Verde et al. 1998a) that the shape dependence of the induced bispectrum (eq. 5) can be used to independently determine  $b_1$  and  $\gamma_2$  from the measured bispectrum.

In order to analyze the theoretical predictions presented

here, following Fry (1984) we define a dimensionless bispectrum

$$Q^r(k_1, \mu, t) = \frac{b_1 B^r(k_1, \mu, t)}{3[P^r(k_1)]^2}. \quad (8)$$

In addition to being dimensionless, this has the added advantage of eliminating the  $b_1$  dependence in eq. (5) which just introduces an overall scaling of the bispectrum. Note that our  $Q^r(k_1, \mu, t)$  is somewhat different from the dimensionless three point hierarchical amplitude  $Q$  used in several earlier works including Fry (1984).

The left panel of Figure 2 shows  $Q^r(\mu, t)$  which refers to  $Q^r(k_1, \mu, t)$  at  $k_1 = 0.2 \text{ Mpc}^{-1}$  for the reference model where  $b_1 = 1$  and  $\gamma_2 = 0$ , and in the subsequent discussion we shall largely focus on the  $(\mu, t)$  dependence for this fixed value of  $k_1$ . The value of  $k_1$  considered here refers to sufficiently large scales where we may expect second order perturbation theory to provide a reasonably valid descriptions. The triangle shapes corresponding to different values of  $(\mu, t)$  has been discussed in Paper I, we summarize this here. The right boundary  $\mu = 1$  corresponds to linear triangles where  $\mathbf{k}_1, -\mathbf{k}_2$  and  $-\mathbf{k}_3$  are parallel (Figure 1). The top right corner ( $\mu \rightarrow 1, t \rightarrow 1$ ) and the bottom right corner ( $\mu \rightarrow 1, t \rightarrow 1/2$ ) correspond to squeezed ( $\mathbf{k}_1 = -\mathbf{k}_2, \mathbf{k}_3 \rightarrow 0$ ) and stretched ( $\mathbf{k}_2 = \mathbf{k}_3 = -\mathbf{k}_1/2$ ) triangles respectively. The top boundary  $t = 1$  corresponds to L-isosceles triangles where the two larger sides ( $\mathbf{k}_1$  and  $\mathbf{k}_2$ ) are of equal length, whereas the bottom boundary  $2\mu t = 1$  corresponds to S-isosceles triangles where the two smaller sides ( $\mathbf{k}_2$  and  $\mathbf{k}_3$ ) are of equal length. The top left corner ( $\mu \rightarrow 1/2, t \rightarrow 1$ ) corresponds to equilateral triangles. The diagonal line  $\mu = t$  corresponds to right-angle triangles ( $\chi = 90^\circ$  in Figure 1) while the upper ( $t > \mu$ ) and lower halves correspond to acute and obtuse triangles respectively.

Considering  $Q^r(\mu, t)$  in the left panel of Figure 2 we see that the value is minimum at the top left corner  $(\mu, t) = (1/2, 1)$  which corresponds to equilateral triangles where

$$Q^r(1/2, 1) = \left(\frac{4}{7} + \gamma_2\right) \quad (9)$$

independent of the value of  $k_1$ . The value of  $Q^r(\mu, t)$  increases as we move away from the equilateral configuration. The corresponding triangle deformation corresponds to increasing  $\chi$  (Figure 1) from  $60^\circ$  to  $180^\circ$ . Equivalently, the value of  $Q^r(\mu, t)$  increases as we change the shape from an acute triangle to an obtuse triangle. The right boundary ( $\mu = 1$ ), where we have the largest values of  $Q^r(\mu, t)$ , corresponds to linear triangles where the three sides of the triangle are aligned. The bottom right corner  $(\mu, t) = (1, 1/2)$  corresponds to stretched triangles, and the top right corner  $(\mu, t) = (1, 1)$  corresponds to squeezed triangles. We see that the maximum value of  $Q^r(\mu, t)$  occurs along the  $\mu = 1$  line close to the squeezed limit. We note that the squeezed triangle where  $|\mathbf{k}_3| \rightarrow 0$  is not straight forward to interpret. In the present analysis we have restricted  $\mathbf{k}_3$  to values which can be probed using a finite observational volume, and the value  $|\mathbf{k}_3| = 0$  where the bispectrum is zero is excluded. The entire discussion of squeezed triangles in this paper is restricted to  $|\mathbf{k}_3| \rightarrow k_{min} = 5 \times 10^{-4} \text{ Mpc}^{-1}$  which is comparable to the horizon scale, and the interpretation is not straightforward as the value of the bispectrum depends on how the triangle is squeezed. If we squeeze a linear triangle

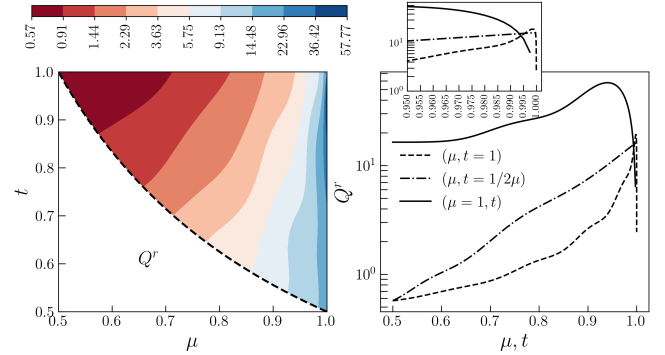


**Figure 2.** Left panel:  $Q^r(\mu, t)$  at  $k_1 = 0.2 \text{ Mpc}^{-1}$  for the reference model where  $b_1 = 1$  and  $\gamma_2 = 0$ . Right panel: The different curves show the values of  $Q^r(\mu, t)$  along the three boundaries of the allowed region of  $(\mu, t)$  space. The  $x$ -axis corresponds to  $\mu$  or  $t$  depending on the curve which is being referred to. The bottom curve shows  $Q^r(\mu, 1)$  as a function of  $\mu$ , this corresponds to L-isosceles triangles (top boundary of left panel). The middle curve shows  $Q^r(\mu, 1/(2\mu))$  as a function of  $\mu$ , this corresponds to S-isosceles triangles (bottom boundary of left panel). The top curve shows  $Q^r(1, t)$  as a function of  $t$ , this corresponds to linear triangles (right boundary of left panel). The inset zooms in on the squeezed limit.

by first setting  $\mu = 1$  and then by taking the limit  $t \rightarrow 1$ , then the values of  $F_{23}$  and  $F_{31}$  diverge (eq. 7), however the diverging parts of these two quantities cancel out to yield a finite value for the bispectrum (eq. 5). In contrast, the values of  $F_{12}, F_{23}$  and  $F_{31}$  are all finite if we squeeze an isosceles triangle where we first set  $t = 1$  and then take the limit  $\mu \rightarrow 1$ . However, the two above mentioned calculations yield different values for the bispectrum. We therefore conclude that the bispectrum does not have a unique value in the squeezed limit, rather the result depends on how one approaches this limit.

The right panel of Figure 2 shows the variation of  $Q^r(\mu, t)$  along the three boundaries of the allowed region of the  $(\mu, t)$  parameter space. The  $x$ -axis corresponds to  $\mu$  or  $t$  depending on the boundary which is being referred to. The bottom dashed curve shows  $Q^r(\mu, 1)$  which corresponds to L-isosceles triangles (top boundary of right panel). The left extremity of this curve ( $\mu = 1/2$ ) corresponds to equilateral triangles whereas the right extremity ( $\mu = 1$ ) corresponds to squeezed triangles. The middle dash-dotted curve shows  $Q^r(\mu, t)$  as a function of  $\mu$  along the boundary  $2\mu t = 1$  which corresponds to S-isosceles triangles. Here also the left extremity ( $\mu = 1/2$ ) corresponds to equilateral triangles whereas now the right extremity ( $\mu = 1$ ) corresponds to stretched triangles. The top solid curve shows  $Q^r(1, t)$  which corresponds to linear triangles (right boundary). Here the left extremity ( $t = 1/2$ ) corresponds to stretched triangles whereas the right extremity ( $t = 1$ ) corresponds to squeezed triangles. The right extremity of the dash-dotted curve and the left extremity of the solid curve both correspond to stretched triangles  $(1, 1/2)$ , and they both correspond to the same value of  $Q^r(\mu, t)$ . The right extremity of the solid curve and the dashed curve both correspond to the squeezed limit. However, as noted earlier the value of the bispectrum depends on how we approach the squeezed limit

and we see that the limiting values are different along these two curves. This is highlighted in the inset of the right panel which provides a zoom-in view of the squeezed limit.

As mentioned earlier, in the right panel also we see that  $Q^r(\mu, t)$  is minimum for the equilateral triangle for which  $\mu = 1/2$ . As  $\mu$  is increased the three sides of the triangle get increasingly more aligned (Figure 1) and the value of  $Q^r(\mu, t)$  increases with the largest values occurring for the linear triangle when the three sides are parallel. We find that the value of  $Q^r(\mu, t)$  increases by a factor of  $\sim 34$  as the equilateral triangle is deformed to a linear triangle ( $\mu = 1$ ) along either of the two lower curves. We find the largest values of  $Q^r(\mu, t)$  along the topmost curve which shows this as a function of  $t$  with  $\mu = 1$ . Considering the variation along the different linear triangles, we find that  $Q^r(\mu, t)$  is nearly constant for  $0.5 \leq t \leq 0.6$ , increases for larger  $t$  and has a maxima at  $t \approx 0.94$  beyond which its value falls. This maxima is close to the squeezed limit where  $k_1 \approx k_2$  and  $k_3 = (1-t)k_1$ . We find that the maximum value of  $Q^r(\mu, t)$  occurs at  $k_3 = k_{eq}$  (matter-radiation equality) which corresponds to the peak of the  $\Lambda$ CDM power spectrum. We have tested this by plotting  $Q^r(\mu, t)$  for other values of  $k_1$  (not shown here). The maximum value of  $Q^r(\mu, t)$  is found to be approximately 100 times larger than the minimum value which occurs for equilateral triangles.

#### 4 INDUCED REDSHIFT SPACE BISPECTRUM

The induced bispectrum in redshift space from second order perturbation theory (Verde et al. 1998b; Scoccimarro et al. 1999b) is given by

$$B^s(\mathbf{k}_1, \mathbf{k}_2, \mathbf{k}_3) = 2b_1^{-1}(1 + \beta_1\mu_1^2)(1 + \beta_1\mu_2^2) \left\{ F_2(\mathbf{k}_1, \mathbf{k}_2) + \frac{\gamma_2}{2} + \mu_3^2\beta_1 G_2(\mathbf{k}_1, \mathbf{k}_2) - b_1\beta_1\mu_3 k_3 \left[ \frac{\mu_1}{k_1}(1 + \beta_1\mu_2^2) + \frac{\mu_2}{k_2}(1 + \beta_1\mu_1^2) \right] \right\} P(k_1)P(k_2) + \text{cyc}..., \quad (10)$$

where  $\beta_1$  is the linear redshift distortion parameter and

$$G_2(k_1, k_2) = \frac{3}{7} + \frac{\mathbf{k}_1 \cdot \mathbf{k}_2}{2} \left( \frac{1}{k_1^2} + \frac{1}{k_2^2} \right) + \frac{4}{7} \frac{(\mathbf{k}_1 \cdot \mathbf{k}_2)^2}{k_1^2 k_2^2}, \quad (11)$$

refers to the second order kernel for the divergence of the peculiar velocity (Goroff et al. 1986). Here we find it useful to use

$$F_2(\mathbf{k}_1, \mathbf{k}_2) = G_2(\mathbf{k}_1, \mathbf{k}_2) + \Delta G(\mathbf{k}_1, \mathbf{k}_2) \quad (12)$$

where

$$\Delta G(\mathbf{k}_1, \mathbf{k}_2) = \frac{2}{7} \left[ 1 - \frac{(\mathbf{k}_1 \cdot \mathbf{k}_2)^2}{k_1^2 k_2^2} \right]. \quad (13)$$

The various terms  $G_2(\mathbf{k}_1, \mathbf{k}_2)$  and  $\Delta G(\mathbf{k}_1, \mathbf{k}_2)$  are dimensionless functions which depend on the shape of the triangle  $(\mathbf{k}_1, \mathbf{k}_2, \mathbf{k}_3)$ , and these have very simple algebraic expressions in terms of  $(\mu, t)$ . Using the compact notation  $G_{12}(\mu, t) = G_2(\mathbf{k}_1, \mathbf{k}_2)$  and  $\Delta G_{12}(\mu, t) = \Delta G(\mathbf{k}_1, \mathbf{k}_2)$ , etc.

we can express these as

$$\begin{aligned} G_{12}(\mu, t) &= \frac{1}{14} \left( 8\mu^2 - 7\mu t - \frac{7\mu}{t} + 6 \right) \\ G_{23}(\mu, t) &= -\frac{6\mu^2 t + t - 7\mu}{14s^2 t} \\ G_{31}(\mu, t) &= \frac{t^2 (-6\mu^2 + 7\mu t - 1)}{14s^2} \end{aligned} \quad (14)$$

and

$$s^2 t^{-2} \Delta G_{31} = s^2 \Delta G_{23} = \Delta G_{12} = \frac{2}{7} (1 - \mu^2). \quad (15)$$

We note that all the  $\Delta G$ s are zero for linear triangles ( $\mu = 1$ ).

For calculating the various angular moments of the redshift space bispectrum we express it as

$$B^s(\hat{\mathbf{p}}, k_1, \mu, t) = 2b_1^{-1} \left\{ R G_{12} + S_{12} \left[ \Delta G_{12} + \frac{\gamma_2}{2} \right] - b_1 T_{12} \right\} P^r(k_1) P^r(k_2) + \text{cyc}... \quad (16)$$

Here the anisotropy or orientation dependence of the redshift space bispectrum is completely quantified by the functions

$$R(\hat{\mathbf{p}}, \beta_1, \mu, t) = (1 + \beta_1\mu_1^2)(1 + \beta_1\mu_2^2)(1 + \beta_1\mu_3^2), \quad (17)$$

$$S_{12}(\hat{\mathbf{p}}, \beta_1, \mu, t) = (1 + \beta_1\mu_1^2)(1 + \beta_1\mu_2^2) \quad (18)$$

and

$$\begin{aligned} T_{12}(\hat{\mathbf{p}}, \beta_1, \mu, t) &= \frac{\beta_1}{2} (1 + \beta_1\mu_1^2)(1 + \beta_1\mu_2^2) \mu_3 k_3 \\ &\times \left[ \frac{\mu_1}{k_1} (1 + \beta_1\mu_2^2) + \frac{\mu_2}{k_2} (1 + \beta_1\mu_1^2) \right]. \end{aligned} \quad (19)$$

The angular multipoles of the redshift space bispectrum can be expressed in terms of the angular multipoles of  $R$ ,  $S_{12}$ ,  $T_{12}$ , etc as

$$\begin{aligned} \bar{B}_\ell^m(k_1, \mu, t) &= 2b_1^{-1} \left\{ \bar{R}_\ell^m G_{12} + [\bar{S}_{12}]_\ell^m \left[ \Delta G_{12} + \frac{\gamma_2}{2} \right] - b_1 [\bar{T}_{12}]_\ell^m \right\} P^r(k_1) P^r(k_2) + \text{cyc}... \end{aligned} \quad (20)$$

where

$$\bar{R}_\ell^m(\beta_1, \mu, t) = \sqrt{\frac{(2\ell+1)}{4\pi}} \int [Y_\ell^m(\hat{\mathbf{p}})]^* R(\hat{\mathbf{p}}, \beta_1, \mu, t) d\Omega_{\hat{\mathbf{p}}}. \quad (21)$$

refers to the angular angular multipoles of  $R(\hat{\mathbf{p}}, \beta_1, \mu, t)$ , and the other multipole moments  $[\bar{S}_{12}]_\ell^m$ ,  $[\bar{T}_{12}]_\ell^m$  etc. have been defined similarly. The different multipole moments  $\bar{R}_\ell^m$ ,  $[\bar{S}_{12}]_\ell^m$ ,  $[\bar{T}_{12}]_\ell^m$  etc. are all polynomials of the form  $c_0 + c_1\beta_1 + c_2\beta_1^2 \dots$  where the smallest power of  $\beta_1$  is  $\ell/2$  and the largest power of  $\beta_1$  is 3, 2 and 4 for  $\bar{R}_\ell^m$ ,  $[\bar{S}_{12}]_\ell^m$  and  $[\bar{T}_{12}]_\ell^m$  respectively. The coefficients of the polynomials depend on  $\ell$ ,  $m$  and the shape of the triangle  $(\mu, t)$ .

$R(\hat{\mathbf{p}}, \beta_1, \mu, t)$  (eq. 17) corresponds to the redshift space enhancement of the bispectrum that arises if each of the three terms  $\Delta(\mathbf{k}_1)$ ,  $\Delta(\mathbf{k}_2)$  and  $\Delta(\mathbf{k}_3)$  in equation (1) is subjected to linear RSD. The angular multipoles  $\bar{R}_\ell^m(\beta_1, \mu, t)$  have non-zero values for even  $\ell$  in the range  $\ell \leq 6$ , while  $m \leq \ell$  with  $m$  being restricted to  $m \leq 4$ . The angular multipoles  $\bar{R}_\ell^m(\beta_1, \mu, t)$  have been studied in detail in Paper I, and when required we use these results here.

Considering the  $S$  terms (eq. 18), the angular multipoles

have non-zero values for even  $\ell$  in the range  $\ell \leq 4$ , while  $m \leq \ell$ . We see that for linear triangles ( $\mu = 1$ ) the three  $S$  terms all reduce to the same value

$$S_{12} = S_{23} = S_{31} = (1 + \beta_1 \mu_1^2)^2. \quad (22)$$

which is exactly the enhancement factor of the power spectrum due to linear RSD. The multipole moments of this enhancement factor have been extensively studied (Hamilton 1997), and denoting these as  $A_\ell$  we have  $A_0 = 1 + 2\beta_1/3 + \beta_1^2/5$ ,  $A_2 = 4(\beta_1/3 + \beta_1^2/7)$  and  $A_4 = 8\beta_1^2/35$ . We find that we can express all the multipole moments with  $m = 0$  in the form

$$[\bar{S}_{12}]_\ell^0(\beta_1, \mu, t) = A_\ell(\beta_1) + \Delta G_{12}(\mu) [C_{12}]_\ell(\beta_1, \mu, t), \quad (23)$$

where the second term in the R.H.S. is zero for linear triangles. Considering the  $S$  terms with  $m \neq 0$ , these are all zero for linear triangles ( $\mu = 1$ ), and we find that we find it convenient to express these in the form

$$[\bar{S}_{12}]_\ell^m(\beta_1, \mu, t) = (1 - \mu^2)^{m/2} [D_{12}]_\ell^m(\beta_1, \mu, t), \quad (24)$$

The expressions needed to calculate the multipole moments of the  $S$  terms ( $A_\ell$ ,  $[C_{12}]_\ell$ ,  $[D_{12}]_\ell$ , etc.) are presented in Appendix A instead of the main body of the text.

Considering the  $T$  terms (eq. 19), the angular multipoles have non-zero values for even  $\ell$  in the range  $\ell \leq 8$ , while  $m \leq \ell$  with  $m \leq 6$ . The expressions for the multipole moments here are rather lengthy and we have presented these in Appendix B instead of the main body of the text.

We have used the multipole moments of  $R$ ,  $S$  and  $T$  in eq. (20) to calculate  $\bar{B}_\ell^m(k_1, \mu, t)$  the multipole moments of the redshift space bispectrum.<sup>1</sup>

## 5 RESULTS

Here we analyze all the non-zero multipole moments of the redshift space bispectrum. For this purpose we shall consider  $Q_\ell^m(k_1, \mu, t)$  which is defined exactly identically as  $Q^r(k_1, \mu, t)$  (eq. 8) except that we have replaced  $B^r(k_1, \mu, t)$  with  $\bar{B}_\ell^m(k_1, \mu, t)$ . Unless mentioned otherwise, we shall focus on  $Q_\ell^0(\mu, t)$  which shows the results for  $k_1 = 0.2 \text{ Mpc}^{-1}$  and the reference model where  $\beta_1 = 1, b_1 = 1$  and  $\gamma_2 = 0$ . Table 1 shows the maximum and minimum values of all the non-zero  $Q_\ell^m(\mu, t)$  along with the  $(\mu, t)$  values where these occur.

The left panel of Figure 3 shows how the dimensionless monopole bispectrum  $Q_0^0(\mu, t)$  varies with the shape of the triangle. We see that the pattern is very similar to that seen in the left panel of Figure 2 for the real space bispectrum  $Q^r(\mu, t)$ . Here also the value is minimum for equilateral triangles, and we have the largest values for linear triangles. For equilateral triangles we have

$$Q_0^0(1/2, 1) = \frac{\beta_1^3}{490} + \frac{\beta_1^2 \gamma_2}{10} + \frac{3\beta_1^2}{35} - \frac{b_1 \beta_1^4}{315} + \frac{b_1 \beta_1^2}{5} + \frac{b_1 \beta_1}{3} + \frac{2\beta_1 \gamma_2}{3} + \frac{3\beta_1}{7} + \gamma_2 + \frac{4}{7} \quad (25)$$

which is independent of  $k_1$ . This goes over to  $Q^r(1/2, 1)$  (eq. 9) for  $\beta = 0$ . Comparing eq. (25) with eq. (20) we

<sup>1</sup> Python scripts for calculating these moments are available at <https://github.com/arindam-mazumdar/rsd-bispec>.

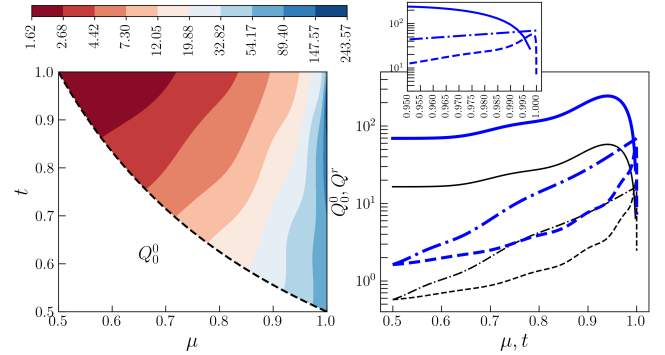


**Figure 3.** Same as Figure 2 except that this shows  $Q_0^0(\mu, t)$ . The right panel shows  $Q^r(\mu, t)$  (black) in addition to  $Q_0^0(\mu, t)$  (blue).

see that the terms involving  $\gamma_2$  arise from the  $S$  terms, the terms involving  $b_1$  arise from the  $T$  terms and the remaining terms are a combination of the contributions from the  $R$  and  $S$  terms. We have checked that our expression for the monopole of the redshift space bispectrum matches the results presented in Scoccimarro et al. (1998a) for the equilateral triangle. A more general comparison is not possible as the parameterization of the triangle shape and size dependence is quite different.

The right panel of Figure 3 is identical to the right panel of Figure 2 except that this shows the monopole  $Q_0^0(\mu, t)$  (blue), the real space bispectrum  $Q^r(\mu, t)$  (black) has also been shown for comparison. We see that the two sets of curves are very similar except for the fact that the values of  $Q_0^0(\mu, t)$  are larger than those of  $Q^r(\mu, t)$ . The enhancement due to RSD is found to be  $\sim 2.8$  for equilateral triangles. Further, we find that the enhancement is minimum for equilateral triangles and it increases as the shape is deformed towards linear triangles. We find that the enhancement is  $\sim 4.2$  for linear triangles irrespective of the value of  $t$ . The location of the maximum value of  $Q_0^0(\mu, t)$  coincides with that of  $Q^r(\mu, t)$ . As discussed earlier, this occurs at  $\mu = 1, t \approx 0.95$  which corresponds to  $k_1 \approx k_2$  and  $k_3 \approx k_{eq}$ . Like the real space bispectrum, we find that the squeezed limit is not uniquely defined for the monopole of the redshift space bispectrum and the result depends on how we approach the squeezed limit. This is highlighted in the inset of the right panel which provides a zoom-in view of the squeezed limit.

Figure 4 shows the  $m = 0$  component of the quadrupole ( $\ell = 2$ ) and all the higher multipoles ( $\ell = 4, 6, 8$ ) which are predicted to have non-zero values. We find that for  $\ell = 2$  and 4 the dependence on the shape of the triangle is very similar to that seen in Figures 2 and 3 for  $Q^r(\mu, t)$  and  $Q_0^0(\mu, t)$  respectively. We have the minimum value for the equilateral triangle, and the value increases as we move towards linear triangles where we have the largest values. Considering  $\ell = 6$  and 8, here also the pattern is similar to that at lower  $\ell$ . We have very small values of  $Q_\ell^0$  in the vicinity of equilateral triangles, and the value increases as we move towards obtuse linear triangles where we have the largest values. The difference, however, is that unlike the lower multipoles we find a region of negative values near the top boundary ( $t = 1$ ). The magnitude of these negative values increases if we ap-

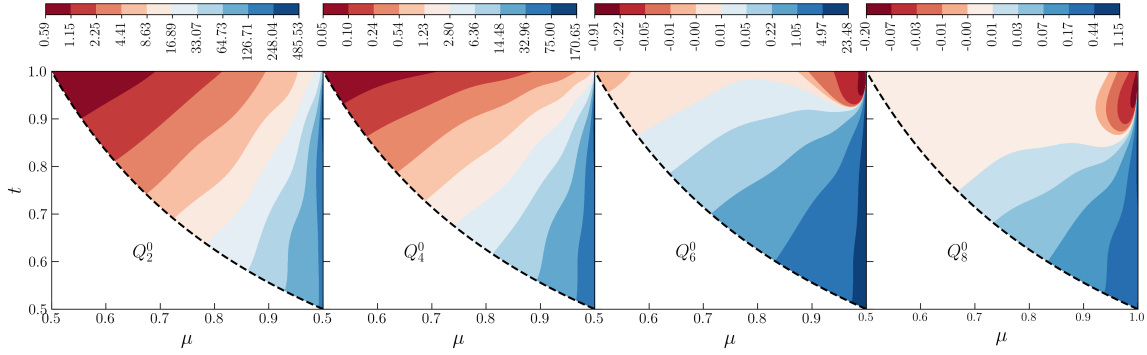


**Figure 4.** Shape dependence of all the  $\ell > 0$  non-zero moments  $Q_\ell^0(\mu, t)$ .

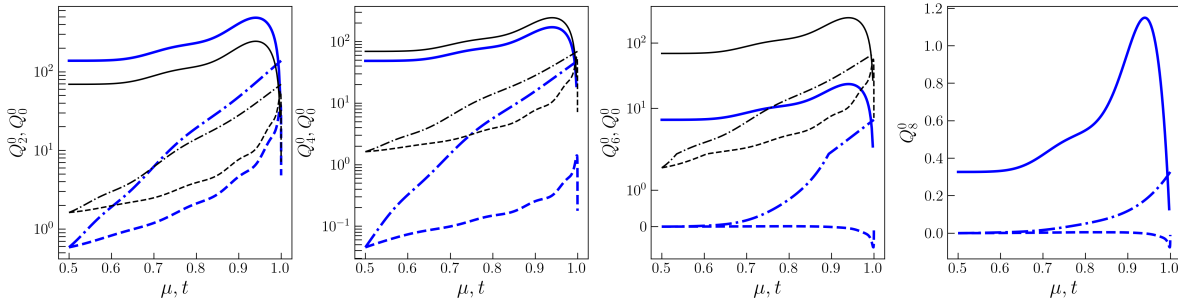


**Figure 5.** Each panel here shows  $Q_\ell^0$  (blue) along the boundaries of the allowed  $(\mu, t)$  region in the corresponding panels of Figure 4,  $Q_0^0$  (black) is also shown for comparison.

proach the squeezed limit along the top boundary, this being particularly pronounced for  $\ell = 8$ .

Figure 5 shows the value of  $Q_\ell^0(\mu, t)$  along the boundaries of the allowed  $(\mu, t)$  region plotted in the different panels of Figure 4. For  $\ell = 2, 4$  and  $6$  the monopole  $Q_0^0(\mu, t)$  is also shown in the respective panels for comparison. We see that the values of  $Q_\ell^0$  get smaller as  $\ell$  is increased (Table 1), and for  $\ell = 8$  the values are so small that it does not make sense to show them together with  $Q_0^0$ . We see that the solid curves which show  $Q_\ell^0(1, t)$  for linear triangles are very similar for all the  $\ell$  values (including  $\ell = 0$ ) shown here. The same is also true for the dashed-dot curves which show  $Q_\ell^0(\mu, 1/(2\mu))$  for the S-isosceles triangles. However, this is not true for the dashed curves which show  $Q_\ell^0(\mu, 1)$  for the L-isosceles triangles. Here  $\ell = 0, 2$ , and  $4$  all show a similar behaviour while  $6$  and  $8$  show a different behaviour where  $Q_\ell^0(\mu, 1)$  has negative values. The various multipole moments with  $\ell > 0$  all quantify the anisotropy or orientation dependence which arises due to RSD, and the ratio  $Q_\ell^m/Q_0^0$  provides a quantitative estimate of the relative strength of this anisotropy. Considering  $m = 0, \ell = 2$  we find that the relative strength of the anisotropy is minimum for equilateral triangles where we have  $Q_2^0(1/2, 1) \approx 0.36 Q_0^0(1/2, 1)$ . The low level of anisotropy for equilateral triangles here may be attributed to the fact that the three vectors  $\mathbf{k}_1, \mathbf{k}_2$  and  $\mathbf{k}_3$  are differently oriented relative to each other. When one of them is aligned with  $\hat{\mathbf{z}}$  for which the RSD is maximum, the other two vector are inclined with respect to  $\hat{\mathbf{z}}$ . We see that the relative strength of the anisotropy increases as the shape is deformed towards linear triangles where the three vectors  $\mathbf{k}_1, \mathbf{k}_2$  and  $\mathbf{k}_3$  are aligned. We have the largest

anisotropy ( $Q_2^0(1, t) \approx 2 Q_0^0(1, t)$ ) for linear triangles irrespective of the value of  $t$ . Interestingly the quadrupole is larger than the monopole ( $Q_2^0 > Q_0^0$ ) over a significant portion of the  $(\mu, t)$  parameter space. As discussed earlier, the maxima of  $Q_2^0(\mu, t)$  occurs at  $\mu = 1, t \approx 0.94$  which corresponds to  $k_1 \approx k_2$  and  $k_3 \approx k_{eq}$ . The position of the maxima coincides with that for  $Q_0^0(\mu, t)$  and  $Q^r(\mu, t)$ . Like the real space bispectrum, we find that the squeezed limit is not uniquely defined for the quadrupole of the redshift space bispectrum and the result depends on how we approach the squeezed limit.  $Q_4^0$  is very similar to  $Q_2^0$  except that the values are smaller with  $Q_4^0(1/2, 1) \approx 0.028 Q_0^0(1/2, 1)$  and  $Q_4^0(1, t) \approx 0.7 Q_0^0(1, t)$  for equilateral and linear triangles respectively. Considering  $\ell = 6$  we find that the values are even smaller with  $Q_6^0(1, t) \approx 0.096 Q_0^0(1, t)$  for linear triangles. The value is negative for equilateral triangles  $Q_6^0(1/2, 1) \approx -0.0019 Q_0^0(1/2, 1)$ , the negative values continue along  $t = 1$  and increases in magnitude as we approach the squeezed limit. However note that the squeezed limit continues to have a positive value if we approach it along  $\mu = 1$ . For  $\ell = 8$  the results are very similar to  $\ell = 6$  except that the values are even smaller with  $Q_8^0(1/2, 1) \approx -0.00035 Q_0^0(1/2, 1)$  and  $Q_8^0(1, t) \approx 0.0047 Q_0^0(1, t)$  for equilateral and linear triangles respectively.

Considering equilateral triangles, we obtain relatively compact expressions for the various  $m = 0$  multipole moments which we present below

$$Q_2^0(1/2, 1) = \frac{\beta_1^3}{588} + \frac{\beta_1^2 \gamma_2}{14} + \frac{3\beta_1^2}{49} - \frac{2}{693} b_1 \beta_1^4 + \frac{b_1 \beta_1^2}{7} + \frac{b_1 \beta_1}{6} + \frac{\beta_1 \gamma_2}{3} + \frac{3\beta_1}{14}, \quad (26)$$

$$Q_4^0(1/2, 1) = \frac{27\beta_1^3}{43120} + \frac{9\beta_1^2\gamma_2}{560} + \frac{27\beta_1^2}{1960} - \frac{27b\beta_1^4}{20020} + \frac{9b\beta_1^2}{280}, \quad (27)$$

$$Q_6^0(1/2, 1) = \frac{59\beta_1^3}{12936} - \frac{1697b\beta_1^4}{221760}, \quad (28)$$

$$Q_6^0(1/2, 1) = -\frac{29b\beta_1^4}{51480}. \quad (29)$$

We have compared our expression for the  $m = 0$  quadrupole moment with the results presented in [Scoccimarro et al. \(1998a\)](#) for the equilateral triangle. We find that the two results match except for the terms involving  $\gamma_2$  for which our results have twice the value. As mentioned earlier, the terms involving  $\gamma_2$  arise from the  $S$  terms (eq. 20). The same  $S$  terms also contribute to the terms which do not have  $\gamma_2$  or  $b_1$ , these however match the results in [Scoccimarro et al. \(1998a\)](#). The cause of this discrepancy is not clear at present. It may however be noted that the different  $m$  components of the multipole moments  $\bar{B}_\ell^m(k_1, \mu, t)$  are not uniquely defined, and these can vary (through a rotation matrix) depending on the choice of  $x, y, z$  axis.

Figures 6 and 7 show all the non-zero  $Q_\ell^m(\mu, t)$  for  $m = 1$  and 2 respectively. We see that the patterns are quite different from those seen in Figures 2, 3 and 4 for  $Q^r(\mu, t)$ ,  $Q_0^0(\mu, t)$  and  $Q_\ell^0(\mu, t)$  respectively. Considering  $m = 1$ , the results are similar for all  $\ell$  values. We see that  $Q_\ell^1(\mu, t)$  is zero for equilateral triangles, and also along the lower boundary (S-isosceles triangles) and the right boundary (linear triangles). We have positive values in the upper left region around the equilateral triangle, the positive region extends along the top of the figure all the way to the squeezed limit. For  $\ell = 2$  we encounter the maximum value of  $Q_2^1(\approx 1)$  at the squeezed limit if we approach it along  $t = 1$ . For higher  $\ell$ , the maximum value is close to the equilibrium triangle and the value gets smaller as  $\ell$  increases.  $Q_\ell^1(\mu, t)$  has negative values for obtuse triangles  $\mu > t$ , and to some extent the negative regions extends across the  $\mu = t$  line into the acute triangles also. The minimum value of  $Q_2^1(\mu, t)$  ( $\approx -70$ ) occurs close to the squeezed limit very near the  $\mu = 1$  boundary (at  $t = 0.95$ ), beyond the minima the value of  $Q_2^1(\mu, t)$  sharply falls to zero at  $\mu = 1$ . The other  $\ell$  values show a similar behaviour, however the magnitude of the minimum value is a factor of 1.7, 9.7 and 155.27 smaller compared to  $\ell = 2$  for  $\ell = 4, 6$  and 8 respectively. Considering  $m = 2$  (Figure 7), for all values of  $\ell$  we find that  $Q_\ell^2(\mu, t)$  has positive values near the squeezed limit with a maxima very close to the squeezed limit beyond which it sharply falls to zero at  $\mu = 1$ .  $Q_2^2(\mu, t)$  is positive everywhere, the maximum value  $\approx 19$  occurs approximately at  $t = 1, \mu = 0.98$  beyond which it sharply falls to zero at  $\mu = 1$ . The location of the maxima is the same for other  $\ell$ , however the value falls by a factor of 1.84, 7.93 and 95.24 compared to  $\ell = 2$  for  $\ell = 4, 6$  and 8 respectively. We see that for all  $\ell$  the minima is near the stretched limit where the values are negative for  $\ell > 2$ . We see that  $Q_\ell^2(\mu, t)$  has a negative value over much of the  $(\mu, t)$  space for  $\ell = 6$  and 8.

Figure 8 shows  $Q_4^m(\mu, t)$  for  $m = 3$  and 4. We see that like  $Q_4^1(\mu, t)$ ,  $Q_4^3(\mu, t)$  also is zero for equilateral triangles, S-isosceles triangles and linear triangles and it has a small positive value ( $\sim 0.1$  and smaller) over much of the  $(\mu, t)$  space. The maximum value ( $\sim 0.2$ ) occurs near the squeezed limit if we approach it close to the top boundary ( $t \approx 1$ ).

$Q_\ell^m$	Maximum $(\mu, t)$	Minimum $(\mu, t)$
$Q_0^0$	243.21 (1, 0.940)	1.62 (0.5, 1)
$Q_2^0$	485.5 (1, 0.940)	0.58 (0.5, 1)
$Q_2^1$	1.124 (0.974, 1)	-68.32 (0.999, 0.956)
$Q_2^2$	19.21 (0.999, 0.980)	0 (1., 0.5)
$Q_4^0$	170.65 (1, 0.940)	0.045 (0.5, 1)
$Q_4^1$	1.557 (0.812, 0.5)	-40.84 (0.999, 0.942)
$Q_4^2$	10.46 (0.999, 0.966)	-0.14 (0.938, 0.533)
$Q_4^3$	0.226 (0.994, 1.0)	-2.08 (0.999, 0.975)
$Q_4^4$	1.22 (0.999, 1.)	0 (1., 0.50)
$Q_6^0$	23.48 (1, 0.94)	-0.83 (0.998, 0.980)
$Q_6^1$	$1.920 \times 10^{-4}$ (0.556, 1.)	-7.06 (0.999, 0.952)
$Q_6^2$	2.42 (0.999, 0.965)	-0.18 (0.929, 0.603)
$Q_6^3$	0.06 (0.972, 0.803)	-0.43 (0.999, 0.979)
$Q_6^4$	$4.308 \times 10^{-3}$ (0.877, 1.)	-0.09 (0.998, 0.977)
$Q_6^5$	$1.586 \times 10^{-3}$ (0.742, 1.)	$-9.172 \times 10^{-3}$ (0.971, 0.917)
$Q_6^6$	$-4.27 \times 10^{-8}$ (0.997, 0.631)	$-7.27 \times 10^{-4}$ (0.724, 0.691)
$Q_8^0$	1.15 (1, 0.940)	-0.18 (0.998, 0.969)
$Q_8^1$	$8.49 \times 10^{-4}$ (0.626, 1.)	-0.44 (0.999, 0.950)
$Q_8^2$	0.20 (0.999, 0.967)	-0.026 (0.920, 0.628)
$Q_8^3$	0.021 (0.974, 0.867)	$-2.09 \times 10^{-4}$ (0.590, 1.)
$Q_8^4$	0.005 (0.774, 0.646)	-0.034 (0.999, 0.996)
$Q_8^5$	0 (0.800, 0.625)	$-5.06 \times 10^{-3}$ (0.974, 0.964)
$Q_8^6$	$-3.61 \times 10^{-9}$ (0.998, 0.502)	$-1.07 \times 10^{-3}$ (0.724, 0.691)

**Table 1.** It shows the maximum and minimum values of all the non-zero  $Q_\ell^m$ .

We find negative values for obtuse triangles ( $\mu > t$ ) near the squeezed limit, and the minimum value ( $\approx -2.08$ ) occurs very close to the squeezed limit ( $\mu = 0.999, t = 0.976$ ). Considering  $Q_4^1(\mu, t)$ , we see that this has positive values over all of  $(\mu, t)$  space, and is zero for linear triangles. The maximum value ( $\approx 1.21$ ) occurs very close to the squeezed limit.

For completeness, we have shown all the remaining non-zero multipoles ( $m = 3, 4, 5, 6$ ) in Figures 9 and 10 for  $\ell = 6$  and 8 respectively. For all the odd  $m$  the value is zero for equilateral and S-isosceles triangles, whereas for linear triangles the value is zero for both odd and even  $m$ . The values of  $Q_\ell^m(\mu, t)$  become extremely small as  $m$  and  $\ell$  are increased, and we have  $|Q_\ell^m(\mu, t)| < 0.1$  for all the results shown in these two figures except for  $Q_6^3$ . We see that  $Q_6^3(\mu, t)$  has relatively larger negative values around the minima ( $\approx -0.43$ ) which occurs for obtuse triangles very close to the squeezed limit.



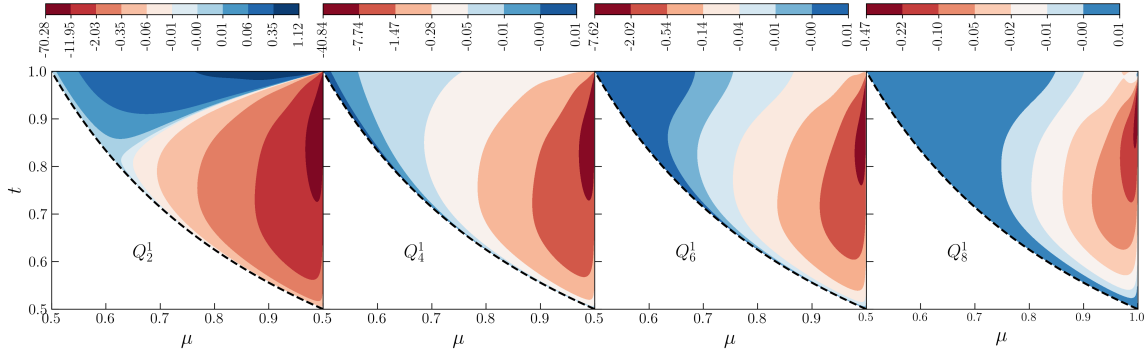


**Figure 6.** Shape dependence of all the non-zero moments  $Q_\ell^1(\mu, t)$ .

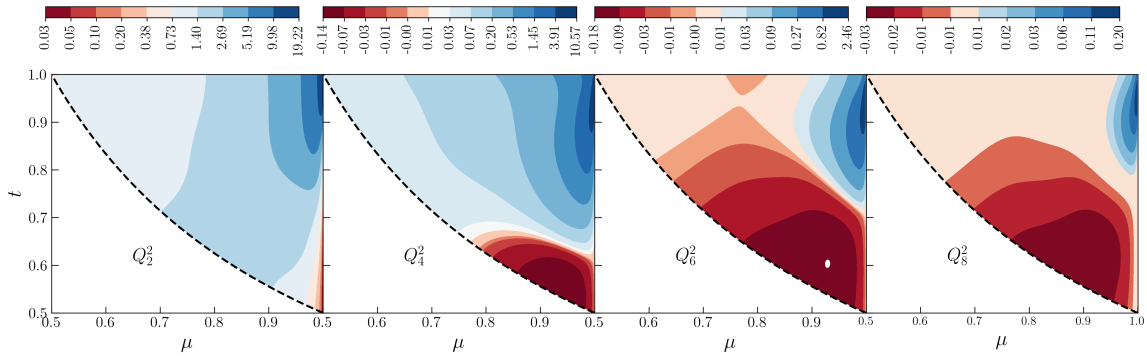


**Figure 7.** Shape dependence of all the non-zero moments  $Q_\ell^2(\mu, t)$ .

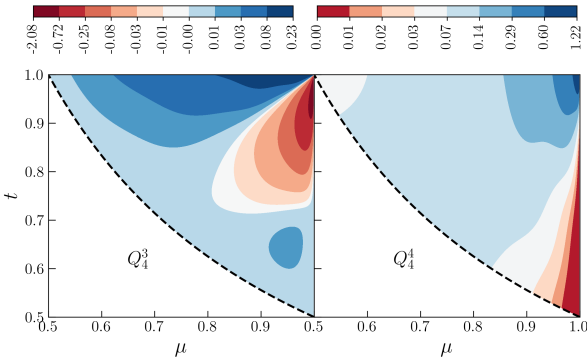


**Figure 8.** Shape dependence of  $Q_4^3(\mu, t)$  and  $Q_4^4(\mu, t)$ .

## 6 SUMMARY AND DISCUSSION

This paper and Paper I together present the formulas needed to calculate all the multipole moments  $\bar{B}_\ell^m(k_1, \mu, t)$  of the redshift space bispectrum which are predicted to be non-zero at second order perturbation theory. Equation (20) represents our final result where the  $R, S$  and  $T$  terms are given in Paper I, Appendices A and B respectively. In this paper we have analyzed  $Q_\ell^m(\mu, t)$  which quantifies the dependence on the shape of the triangle keeping the other quantities which affect  $\bar{B}_\ell^m(k_1, \mu, t)$  fixed at  $k_1 = 0.2 \text{ Mpc}^{-1}$ ,  $\beta_1 = 1, b_1 = 1, \gamma_2 = 0$ . The results are not very different for other values of  $k_1$  close to  $0.2 \text{ Mpc}^{-1}$ . We have also analyzed  $Q^r(\mu, t)$  which corresponds to the real space bispectrum.

We find that  $Q^r(\mu, t), Q_0^0(\mu, t), Q_2^0(\mu, t)$  and  $Q_4^0(\mu, t)$  all show very similar behaviour where the values are positive everywhere, we have the smallest value for equilateral triangles, the value increases as the triangle is deformed towards a linear triangle and we have the largest values for linear triangles. In all of these cases we have the maximum value at  $\mu = 1, t \approx 0.94$  which is very close to the squeezed limit and where  $k_1 \approx k_2$  with  $k_3 \approx k_{eq}$ . Considering any triangle shape  $(\mu, t)$  the monopole  $Q_0^0$  exceeds  $Q^r$ , the RSD enhancement being minimum for equilateral and maximum for linear triangles. The quadrupole  $Q_2^0$  exceeds  $Q_0^0$  for a significant region of  $(\mu, t)$  space in the proximity of linear triangles, however  $Q_2^0$  is smaller than  $Q_0^0$  around the equilateral configuration. The values of  $Q_4^0$  are smaller than those of  $Q_0^0$  for the entire  $(\mu, t)$  space, the two differing by a factor of 3 and 30 for linear and equilateral triangles respectively. The  $m = 1$  and  $m = 2$  multipoles show distinctly different patterns. For  $Q_2^1$  we have negative values of large magnitude near the squeezed limit for obtuse triangles, and the maximum magnitude is roughly 4 times smaller than the maxima of  $Q_0^0$ .  $Q_2^2$  is positive throughout, and has a maxima very close to the squeezed limit with maximum value  $\approx 13$  times smaller than the maxima of  $Q_0^0$ . The higher multipoles all show a rich variety of shape dependence, however the values of  $|Q_\ell^m|$  falls drastically as  $\ell$  and  $m$  are increased.

The various patterns in the shape dependence of  $Q_\ell^m(\mu, t)$  shown here are purely a consequence of non-linear gravitational clustering as we have used  $\gamma_2 = 0$  throughout. Non-linear bias ( $\gamma_2 \neq 0$ ), if present, will cause the shape dependence of  $Q_\ell^m(\mu, t)$  to differ from that shown here. The

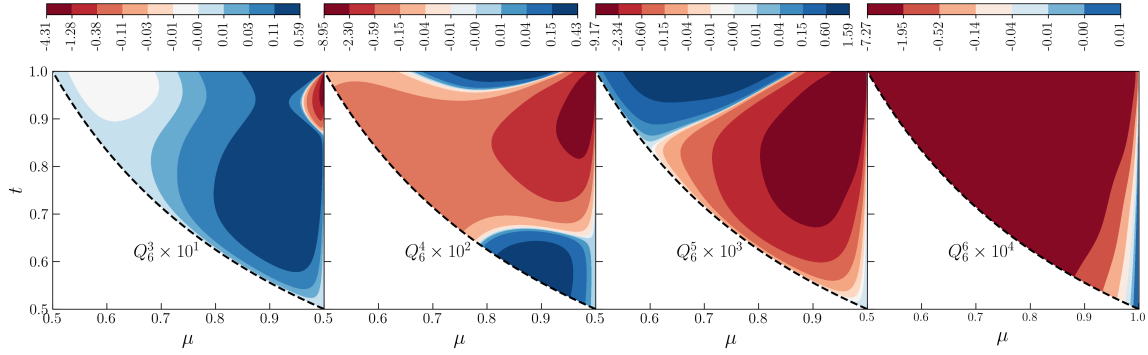


**Figure 9.** Shape dependence of all the  $m > 2$  non-zero moments  $Q_6^m(\mu, t)$ .

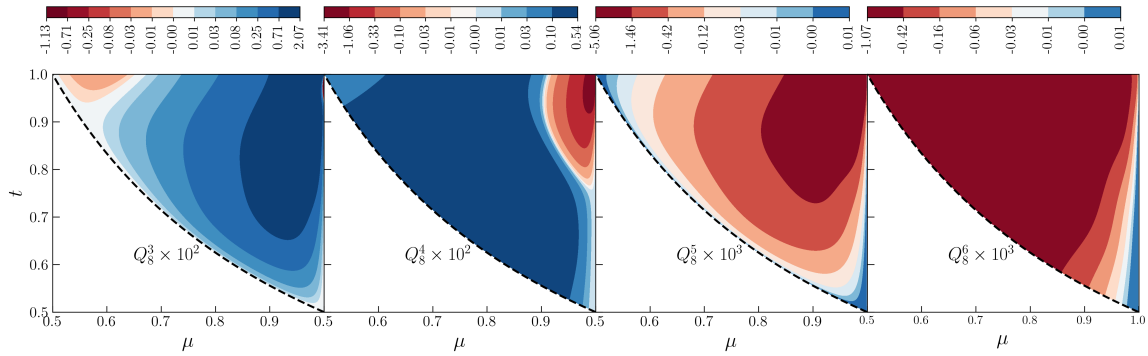


**Figure 10.** Shape dependence of all the  $m > 2$  non-zero moments  $Q_8^m(\mu, t)$ .

$k_1$  and shape  $(\mu, t)$  dependence of the various multipole moments of the bispectrum contains a wealth of cosmological information. It has been proposed that the shape dependence of the bispectrum can be used to determine the parameters  $\beta_1, b_1$  and  $\gamma_2$ . We propose to study these issues in future.

Upcoming future galaxy surveys like Euclid (Laureijs et al. 2011) and DESI (Levi et al. 2013) are aimed to cover large volumes of the order of several Gpc<sup>3</sup>. Following Scoccimarro et al. (1998b) (and also Tellarini et al. 2016) we have estimated the expected variance of the bispectrum for such surveys. Expressing this in terms of  $Q$  we obtain  $\Delta Q \approx 0.001$  for equilateral triangles with  $k_1 = 0.2 \text{ Mpc}^{-1}$  and bin width  $(\delta k_1) = k_1/10$ . These estimates indicate that in future it may be possible to observe a large number of the bispectrum multipoles considered here (Table 1) all the way to  $Q_6^4$  or  $Q_6^5$ . In subsequent works we plan to present more quantitative predictions for observing these multipoles.

## ACKNOWLEDGEMENTS

DS acknowledges support from the Azrieli Foundation for his Postdoctoral Fellowship.

## DATA AVAILABILITY

The data underlying this article were generated by the sources available in public domain

[https://lesgourg.github.io/class\\_public/class.html](https://lesgourg.github.io/class_public/class.html) and <https://github.com/arindam-mazumdar/rsd-bispec>

## REFERENCES

- Ballardini M., Matthewson W. L., Maartens R., 2019, arXiv e-prints, p. arXiv:1906.04730
- Baumann D., 2009, arXiv e-prints, p. arXiv:0907.5424
- Bharadwaj S., Mazumdar A., Sarkar D., 2020, *Mon. Not. Roy. Astron. Soc.*, 493, 594
- Blas D., Lesgourgues J., Tram T., 2011, *JCAP*, 07, 034
- Clarkson C., de Weerd E. M., Jolicœur S., Maartens R., Umeh O., 2019, *Mon. Not. Roy. Astron. Soc.*, 486, L101
- Desjacques V., Jeong D., Schmidt F., 2018, *J. Cosmology Astropart. Phys.*, 12, 035
- Feldman H. A., Frieman J. A., Fry J. N., Scoccimarro R., 2001, *Physical Review Letters*, 86, 1434
- Fergusson J. R., Liguori M., Shellard E. P. S., 2012, *J. Cosmology Astropart. Phys.*, 12, 032
- Fry J. N., 1984, *ApJ*, 279, 499
- Gil-Marín H., Noreña J., Verde L., Percival W. J., Wagner C., Manera M., Schneider D. P., 2015, *MNRAS*, 451, 539
- Goroff M. H., Grinstein B., Rey S. J., Wise M. B., 1986, *Astrophys. J.*, 311, 6
- Galdi D., Verde L., 2020, arXiv e-prints, p. arXiv:2003.12075
- Guzzo L., et al., 2008, *Nature*, 451, 541
- Hamilton A. J. S., 1997, in Ringberg Workshop on Large Scale Structure Ringberg, Germany, September 23-28, 1996. (arXiv:astro-ph/9708102), doi:10.1007/978-94-011-4960-0\_17
- Hamilton A. J. S., 1998, in Hamilton D., ed., *Astrophysics*

and Space Science Library Vol. 231, The Evolving Universe. p. 185 ([arXiv:astro-ph/9708102](https://arxiv.org/abs/astro-ph/9708102)), [doi:10.1007/978-94-011-4960-0-17](https://doi.org/10.1007/978-94-011-4960-0-17)

Hashimoto I., Rasera Y., Taruya A., 2017, *Phys. Rev. D*, **96**, 043526

Hawkins E., et al., 2003, *MNRAS*, **346**, 78

Hivon E., Bouchet F. R., Colombi S., Juszkiewicz R., 1995, *A&A*, **298**, 643

Hu W., Eisenstein D. J., Tegmark M., 1998, *Phys. Rev. Lett.*, **80**, 5255

Jackson J. C., 1972, *MNRAS*, **156**, 1P

Johnson A., Blake C., Dossett J., Koda J., Parkinson D., Joudaki S., 2016, *MNRAS*, **458**, 2725

Kaiser N., 1987, *MNRAS*, **227**, 1

Laureijs R., et al., 2011, arXiv e-prints, p. [arXiv:1110.3193](https://arxiv.org/abs/1110.3193)

Lesgourgues J., 2011, arXiv e-prints, p. [arXiv:1104.2932](https://arxiv.org/abs/1104.2932)

Levi M., et al., 2013, [arXiv:1308.0847](https://arxiv.org/abs/1308.0847)

Liguori M., Sefusatti E., Fergusson J. R., Shellard E. P. S., 2010, *Advances in Astronomy*, **2010**, 980523

Linder E. V., 2008, *Astroparticle Physics*, **29**, 336

Loveday J., Efstathiou G., Maddox S. J., Peterson B. A., 1996, *ApJ*, **468**, 1

Matarrese S., Verde L., Heavens A. F., 1997, *MNRAS*, **290**, 651

Mueller E.-M., Percival W., Linder E., Alam S., Zhao G.-B., Sánchez A. G., Beutler F., Brinkmann J., 2018, *MNRAS*, **475**, 2122

Nan Y., Yamamoto K., Hikage C., 2018, *J. Cosmology Astropart. Phys.*, **07**, 038

Nishimichi T., Kayo I., Hikage C., Yahata K., Taruya A., Jing Y. P., Sheth R. K., Suto Y., 2007, *PASJ*, **59**, 93

Oppizzi F., Liguori M., Renzi A., Arroja F., Bartolo N., 2018, *J. Cosmology Astropart. Phys.*, **05**, 045

Peacock J. A., et al., 2001, *Nature*, **410**, 169

Planck Collaboration et al., 2016, *A&A*, **594**, A13

Planck Collaboration et al., 2019, arXiv e-prints, p. [arXiv:1905.05697](https://arxiv.org/abs/1905.05697)

Scoccimarro R., Colombi S., Fry J. N., Frieman J. A., Hivon E., Melott A., 1998a, *ApJ*, **496**, 586

Scoccimarro R., Colombi S., Fry J. N., Frieman J. A., Hivon E., Melott A., 1998b, *Astrophys. J.*, **496**, 586

Scoccimarro R., Couchman H. M. P., Frieman J. A., 1999a, *ApJ*, **517**, 531

Scoccimarro R., Couchman H. M. P., Frieman J. A., 1999b, *Astrophys. J.*, **517**, 531

Scoccimarro R., Feldman H. A., Fry J. N., Frieman J. A., 2001, *ApJ*, **546**, 652

Scoccimarro R., Sefusatti E., Zaldarriaga M., 2004, *Phys. Rev. D*, **69**, 103513

Shiraishi M., 2019, *Frontiers in Astronomy and Space Sciences*, **6**, 49

Slepian Z., Eisenstein D. J., 2017, *Mon. Not. Roy. Astron. Soc.*, **469**, 2059

Slepian Z., Eisenstein D. J., 2018, *MNRAS*, **478**, 1468

Song Y.-S., Percival W. J., 2009, *J. Cosmology Astropart. Phys.*, **10**, 004

Sugiyama N. S., Saito S., Beutler F., Seo H.-J., 2019, *MNRAS*, **484**, 364

Tellarini M., Ross A. J., Tasinato G., Wands D., 2016, *JCAP*, **06**, 014

Upadhye A., 2019, *JCAP*, **05**, 041

Verde L., Heavens A. F., Matarrese S., Moscardini L., 1998a, *MNRAS*, **300**, 747

Verde L., Heavens A. F., Matarrese S., Moscardini L., 1998b, *Mon. Not. Roy. Astron. Soc.*, **300**, 747

Verde L., Heavens A. F., Matarrese S., Moscardini L., 1998c, *MNRAS*, **300**, 747

Verde L., et al., 2002, *MNRAS*, **335**, 432

Yankelevich V., Porciani C., 2019, *MNRAS*, **483**, 2078

de Weerd E. M., Clarkson C., Jolicoeur S., Maartens R., Umeh O., 2020, *JCAP*, **05**, 018

de la Torre S., et al., 2017, *Astron. Astrophys.*, **608**, A44

## APPENDIX A: MULTIPOLE MOMENTS OF THE $S$ TERMS

$$A_0 = 1 + 2\beta_1/3 + \beta_1^2/5 \quad (\text{A1})$$

$$A_2 = 4(\beta_1/3 + \beta_1^2/7) \quad (\text{A2})$$

$$A_4 = 8\beta_1^2/35 \quad (\text{A3})$$

$$[C_{12}]_0 = [C_{23}]_0 = [C_{31}]_0 = -\frac{7\beta_1^2}{15}. \quad (\text{A4})$$

$$[C_{12}]_2 = [C_{31}]_2 = -\frac{1}{6}\beta_1(11\beta_1 + 21) \quad (\text{A5})$$

$$[C_{23}]_2 = -\frac{1}{6}\beta_1(11\beta_1 + 6(3\beta_1 + 7)t^2 - 6(3\beta_1 + 7)\mu t + 21). \quad (\text{A6})$$

$$[C_{31}]_4 = [C_{12}]_4 = -\frac{6\beta_1^2}{5} \quad (\text{A7})$$

$$[C_{23}]_4 = -\frac{1}{10}\beta_1^2(5(7\mu^2 + 1)t^2 - 40\mu t + 12) \quad (\text{A8})$$

$$[D_{12}]_2^1 = \frac{1}{7}\sqrt{\frac{2}{3}}\beta_1(3\beta_1 + 7)\mu, \quad (\text{A9})$$

$$[D_{23}]_2^1 = \sqrt{\frac{2}{3}}\frac{\beta_1}{7s^2}[\mu(3\beta_1 + 7s^2) + (6\beta_1 + 7)\mu t^2 - t(\beta_1(6\mu^2 + 3) + 7)] \quad (\text{A10})$$

$$[D_{31}]_2^1 = \frac{\sqrt{\frac{2}{3}}\beta_1(3\beta_1 + 7)t(\mu t - 1)}{7s^2}. \quad (\text{A11})$$

$$[D_{12}]_2^2 = \frac{\beta_1(\beta_1 + 7)}{7\sqrt{6}}, \quad (\text{A12})$$

$$[D_{23}]_2^2 = \frac{\beta_1(\beta_1 + 7s^2 + (6\beta_1 + 7)t^2 - 6\beta_1\mu t)}{7\sqrt{6}s^2} \quad (\text{A13})$$

$$[D_{31}]_2^2 = \frac{\beta_1(\beta_1 + 7)t^2}{7\sqrt{6}s^2}. \quad (\text{A14})$$

$$[D_{12}]_4^1 = \frac{4\beta_1^2\mu}{7\sqrt{5}} \quad (\text{A15})$$

$$[D_{23}]_4^1 = \frac{\beta_1^2(2\mu t - 1)((7\mu^2 - 3)t - 4\mu)}{7\sqrt{5}s^2} \quad (\text{A16})$$

$$[D_{31}]_4^1 = \frac{4\beta_1^2 t(\mu t - 1)}{7\sqrt{5}s^2} \quad (\text{A17})$$

$$[D_{12}]_4^2 = \frac{1}{7}\sqrt{\frac{2}{5}}\beta_1^2 \quad (\text{A18})$$

$$[D_{23}]_4^2 = \frac{\sqrt{\frac{2}{5}}\beta_1^2 ((7\mu^2 - 1)t^2 - 6\mu t + 1)}{7s^2} \quad (\text{A19})$$

$$[D_{31}]_4^2 = \frac{\sqrt{\frac{2}{5}}\beta_1^2 t^2}{7s^2} \quad (\text{A20})$$

$$[D_{23}]_4^3 = \frac{\beta_1^2 t(2\mu t - 1)}{\sqrt{35}s^2} \quad (\text{A21})$$

$$[D_{23}]_4^4 = \frac{\beta_1^2 t^2}{\sqrt{70}s^2} \quad (\text{A22})$$

$[D_{12}]_4^3, [D_{31}]_4^3, [D_{12}]_4^4, [D_{31}]_4^4$  are zero.

## APPENDIX B: MULTIPOLE MOMENTS OF THE $T$ TERMS

$$\begin{aligned} [\bar{T}_{12}]_0^0 = & -\frac{8}{315}\beta^4\mu^4 - \frac{8\beta^4\mu^2}{105} - \frac{\beta^4}{105} - \frac{12\beta^3\mu^2}{35} - \frac{3\beta^3}{35} \\ & - \frac{4\beta^2\mu^2}{15} - \frac{\beta^2}{3} - \frac{\beta}{3} + \frac{2}{63}\beta^4\mu^3 t + \frac{2\beta^4\mu^3}{63t} \\ & + \frac{1}{42}\beta^4\mu t + \frac{\beta^4\mu}{42t} + \frac{2}{35}\beta^3\mu^3 t + \frac{2\beta^3\mu^3}{35t} + \frac{11}{70}\beta^3\mu t \\ & + \frac{11\beta^3\mu}{70t} + \frac{3}{10}\beta^2\mu t + \frac{3\beta^2\mu}{10t} + \frac{\beta\mu t}{6} + \frac{\beta\mu}{6t} \end{aligned} \quad (\text{B1})$$

$$\begin{aligned} [\bar{T}_{23}]_0^0 = & \frac{4\beta^4\mu^4}{105s^4} + \frac{4\beta^4\mu^2}{35s^4} + \frac{\beta^4}{70s^4} + \frac{4\beta^3\mu^2}{35s^4} + \frac{\beta^3}{35s^4} - \frac{\beta^2}{10s^4} \\ & + \frac{\beta^3\mu t^3}{14s^4} + \frac{\beta^2\mu t^3}{10s^4} + \frac{\beta^4\mu^2 t^2}{21s^4} + \frac{\beta^4 t^2}{126s^4} - \frac{4\beta^3\mu^2 t^2}{35s^4} \\ & - \frac{\beta^3 t^2}{35s^4} - \frac{\beta^2\mu^2 t^2}{5s^4} - \frac{\beta^2 t^2}{10s^4} - \frac{2\beta^4\mu^3 t}{21s^4} - \frac{2\beta^4\mu^3}{63s^4 t} \\ & - \frac{\beta^4\mu t}{14s^4} - \frac{\beta^4\mu}{42s^4 t} - \frac{\beta^3\mu}{14s^4 t} + \frac{3\beta^2\mu t}{10s^4} + \frac{6\beta^3\mu^2}{35s^2} \\ & + \frac{3\beta^3}{70s^2} + \frac{2\beta^2\mu^2}{15s^2} + \frac{\beta^2}{15s^2} - \frac{\beta}{6s^2} - \frac{2\beta^3\mu^3}{35s^2 t} \\ & - \frac{\beta^3\mu t}{14s^2} - \frac{3\beta^3\mu}{35s^2 t} - \frac{\beta^2\mu}{5s^2 t} + \frac{\beta\mu t}{6s^2} - \frac{\beta^2\mu}{10t} - \frac{\beta\mu}{6t} \end{aligned} \quad (\text{B2})$$

$$\begin{aligned} [\bar{T}_{31}]_0^0 = & -\frac{2\beta^4\mu^3 t^5}{63s^4} - \frac{\beta^4\mu t^5}{42s^4} - \frac{\beta^3\mu t^5}{14s^4} + \frac{4\beta^4\mu^4 t^4}{105s^4} + \frac{4\beta^4\mu^2 t^4}{35s^4} \\ & + \frac{\beta^4 t^4}{70s^4} + \frac{4\beta^3\mu^2 t^4}{35s^4} + \frac{\beta^3 t^4}{35s^4} - \frac{\beta^2 t^4}{10s^4} - \frac{2\beta^4\mu^3 t^3}{21s^4} \\ & - \frac{\beta^4\mu t^3}{14s^4} + \frac{3\beta^2\mu t^3}{10s^4} + \frac{\beta^4\mu^2 t^2}{21s^4} + \frac{\beta^4 t^2}{126s^4} - \frac{4\beta^3\mu^2 t^2}{35s^4} \\ & - \frac{\beta^3 t^2}{35s^4} - \frac{\beta^2\mu^2 t^2}{5s^4} - \frac{\beta^2 t^2}{10s^4} + \frac{\beta^3\mu t}{14s^4} + \frac{\beta^2\mu t}{10s^4} - \frac{2\beta^3\mu^3 t^3}{35s^2} \\ & - \frac{3\beta^3\mu t^3}{35s^2} - \frac{\beta^2\mu t^3}{5s^2} + \frac{6\beta^3\mu^2 t^2}{35s^2} + \frac{3\beta^3 t^2}{70s^2} + \frac{2\beta^2\mu^2 t^2}{15s^2} \\ & + \frac{\beta^2 t^2}{15s^2} - \frac{\beta t^2}{6s^2} - \frac{\beta^3\mu t}{14s^2} + \frac{\beta\mu t}{6s^2} - \frac{1}{10}\beta^2\mu t - \frac{\beta\mu t}{6} \end{aligned} \quad (\text{B3})$$

$$\begin{aligned} [\bar{T}_{12}]_2^0 = & -\frac{136\beta^4\mu^4}{693} - \frac{46\beta^4\mu^2}{231} - \frac{2\beta^4}{231} - \frac{2\beta^3\mu^4}{7} - \frac{15\beta^3\mu^2}{14} \\ & - \frac{\beta^3}{14} - \frac{31\beta^2\mu^2}{21} - \frac{5\beta^2}{21} - \frac{\beta\mu^2}{2} - \frac{\beta}{6} + \frac{10}{231}\beta^4\mu^5 t \\ & + \frac{95}{693}\beta^4\mu^3 t + \frac{205\beta^4\mu^3}{1386t} + \frac{5}{231}\beta^4\mu t + \frac{25\beta^4\mu}{462t} \\ & + \frac{4}{7}\beta^3\mu^3 t + \frac{\beta^3\mu^3}{3t} + \frac{1}{7}\beta^3\mu t + \frac{8\beta^3\mu}{21t} + \frac{3}{7}\beta^2\mu^3 t \\ & + \frac{3\beta^2\mu^3}{14t} + \frac{3}{7}\beta^2\mu t + \frac{9\beta^2\mu}{14t} + \frac{\beta\mu t}{3} + \frac{\beta\mu}{3t} \end{aligned} \quad (\text{B4})$$

$$\begin{aligned} [\bar{T}_{23}]_2^0 = & \frac{68\beta^4\mu^4}{231s^4} + \frac{23\beta^4\mu^2}{77s^4} + \frac{\beta^4}{77s^4} + \frac{3\beta^3\mu^2}{7s^4} + \frac{\beta^3}{21s^4} - \frac{2\beta^2}{7s^4} \\ & + \frac{5\beta^3\mu^3 t^3}{21s^4} + \frac{3\beta^2\mu^3 t^3}{14s^4} + \frac{\beta^2\mu t^3}{14s^4} + \frac{10\beta^4\mu^4 t^2}{77s^4} \\ & + \frac{5\beta^4\mu^2 t^2}{66s^4} - \frac{5\beta^4 t^2}{1386s^4} - \frac{4\beta^3\mu^4 t^2}{21s^4} - \frac{2\beta^3\mu^2 t^2}{7s^4} \\ & - \frac{11\beta^2\mu^2 t^2}{14s^4} - \frac{\beta^2 t^2}{14s^4} - \frac{10\beta^4\mu^5 t}{77s^4} - \frac{95\beta^4\mu^3 t}{231s^4} \\ & - \frac{205\beta^4\mu^3}{1386s^4 t} - \frac{5\beta^4\mu t}{77s^4} - \frac{25\beta^4\mu}{462s^4 t} - \frac{5\beta^3\mu}{21s^4 t} + \frac{6\beta^2\mu t}{7s^4} \\ & + \frac{2\beta^3\mu^4}{7s^2} + \frac{3\beta^3\mu^2}{7s^2} + \frac{11\beta^2\mu^2}{21s^2} + \frac{\beta^2}{21s^2} - \frac{\beta}{3s^2} - \frac{5\beta^3\mu^3 t}{21s^2} \\ & - \frac{\beta^3\mu^3}{3s^2 t} - \frac{\beta^3\mu}{7s^2 t} - \frac{4\beta^2\mu}{7s^2 t} + \frac{\beta\mu t}{3s^2} - \frac{3\beta^2\mu^3}{14t} - \frac{\beta^2\mu}{14t} - \frac{\beta\mu}{3t} \end{aligned} \quad (\text{B5})$$

$$\begin{aligned} [\bar{T}_{31}]_2^0 = & -\frac{10\beta^4\mu^5 t^5}{231s^4} - \frac{95\beta^4\mu^3 t^5}{693s^4} - \frac{5\beta^4\mu t^5}{231s^4} - \frac{5\beta^3\mu^3 t^5}{21s^4} \\ & + \frac{68\beta^4\mu^4 t^4}{231s^4} + \frac{23\beta^4\mu^2 t^4}{77s^4} + \frac{\beta^4 t^4}{77s^4} + \frac{4\beta^3\mu^4 t^4}{21s^4} \\ & + \frac{2\beta^3\mu^2 t^4}{7s^4} - \frac{3\beta^2\mu^2 t^4}{7s^4} + \frac{\beta^2 t^4}{7s^4} - \frac{205\beta^4\mu^3 t^3}{462s^4} \\ & - \frac{25\beta^4\mu t^3}{154s^4} + \frac{9\beta^2\mu^3 t^3}{14s^4} + \frac{3\beta^2\mu t^3}{14s^4} + \frac{85\beta^4\mu^2 t^2}{462s^4} \\ & + \frac{25\beta^4 t^2}{1386s^4} - \frac{3\beta^3\mu^2 t^2}{7s^4} - \frac{\beta^3 t^2}{21s^4} - \frac{11\beta^2\mu^2 t^2}{14s^4} - \frac{\beta^2 t^2}{14s^4} \\ & + \frac{5\beta^3\mu t}{21s^4} + \frac{2\beta^2\mu t}{7s^4} - \frac{\beta^3\mu^3 t^3}{3s^2} - \frac{\beta^3\mu t^3}{7s^2} - \frac{3\beta^2\mu^3 t^3}{7s^2} \\ & - \frac{\beta^2\mu t^3}{7s^2} + \frac{9\beta^3\mu^2 t^2}{14s^2} + \frac{\beta^3 t^2}{14s^2} + \frac{11\beta^2\mu^2 t^2}{21s^2} + \frac{\beta^2 t^2}{21s^2} \\ & - \frac{\beta\mu^2 t^2}{2s^2} + \frac{\beta t^2}{6s^2} - \frac{5\beta^3\mu t}{21s^2} + \frac{\beta\mu t}{3s^2} - \frac{2}{7}\beta^2\mu t - \frac{\beta\mu t}{3} \end{aligned} \quad (\text{B6})$$

$$\begin{aligned}
 [\bar{T}_{12}]_2^1 = & \sqrt{1-\mu^2} \left\{ -\frac{40}{231} \sqrt{\frac{2}{3}} \beta^4 \mu^3 - \frac{10}{77} \sqrt{\frac{2}{3}} \beta^4 \mu \right. \\
 & - \frac{2}{7} \sqrt{\frac{2}{3}} \beta^3 \mu^3 - \frac{11\beta^3 \mu}{7\sqrt{6}} - \frac{3}{7} \sqrt{6} \beta^2 \mu - \frac{\beta \mu}{\sqrt{6}} \\
 & + \frac{10}{231} \sqrt{\frac{2}{3}} \beta^4 \mu^4 t + \frac{10}{77} \sqrt{\frac{2}{3}} \beta^4 \mu^2 t + \frac{5\sqrt{\frac{3}{2}} \beta^4 \mu^2}{77t} \\
 & + \frac{5\beta^4 t}{154\sqrt{6}} + \frac{5\beta^4}{154\sqrt{6}t} + \frac{11}{21} \sqrt{\frac{2}{3}} \beta^3 \mu^2 t + \frac{2\sqrt{\frac{3}{2}} \beta^3 \mu^2}{7t} \\
 & + \frac{11\beta^3 t}{42\sqrt{6}} + \frac{11\beta^3}{42\sqrt{6}t} + \frac{1}{7} \sqrt{6} \beta^2 \mu^2 t + \frac{\sqrt{\frac{3}{2}} \beta^2 \mu^2}{7t} \\
 & \left. + \frac{3}{14} \sqrt{\frac{3}{2}} \beta^2 t + \frac{3\sqrt{\frac{3}{2}} \beta^2}{14t} + \frac{\beta t}{2\sqrt{6}} + \frac{\beta}{2\sqrt{6}t} \right\}
 \end{aligned}
 \tag{B7}$$

$$\begin{aligned}
 [\bar{T}_{23}]_2^1 = & \sqrt{1-\mu^2} \left\{ \frac{20\sqrt{\frac{2}{3}} \beta^4 \mu^3}{77s^4} + \frac{5\sqrt{6} \beta^4 \mu}{77s^4} + \frac{5\sqrt{\frac{2}{3}} \beta^3 \mu}{21s^4} \right. \\
 & + \frac{5\sqrt{\frac{2}{3}} \beta^3 \mu^2 t^3}{21s^4} + \frac{5\beta^3 t^3}{42\sqrt{6}s^4} + \frac{\sqrt{\frac{3}{2}} \beta^2 \mu^2 t^3}{7s^4} \\
 & + \frac{\sqrt{\frac{3}{2}} \beta^2 t^3}{14s^4} + \frac{10\sqrt{\frac{2}{3}} \beta^4 \mu^3 t^2}{77s^4} + \frac{5\sqrt{\frac{3}{2}} \beta^4 \mu t^2}{77s^4} \\
 & - \frac{4\sqrt{\frac{2}{3}} \beta^3 \mu^3 t^2}{21s^4} - \frac{2\sqrt{\frac{2}{3}} \beta^3 \mu t^2}{7s^4} - \frac{3\sqrt{\frac{3}{2}} \beta^2 \mu^2 t^2}{7s^4} \\
 & - \frac{10\sqrt{\frac{2}{3}} \beta^4 \mu^4 t}{77s^4} - \frac{10\sqrt{6} \beta^4 \mu^2 t}{77s^4} - \frac{5\sqrt{\frac{3}{2}} \beta^4 \mu^2}{77s^4 t} \\
 & - \frac{5\sqrt{\frac{3}{2}} \beta^4 t}{154s^4} - \frac{5\beta^4}{154\sqrt{6}s^4 t} - \frac{5\beta^3}{42\sqrt{6}s^4 t} + \frac{3\sqrt{\frac{3}{2}} \beta^2 t}{14s^4} \\
 & + \frac{2\sqrt{\frac{2}{3}} \beta^3 \mu^3}{7s^2} + \frac{\sqrt{6} \beta^3 \mu}{7s^2} + \frac{\sqrt{6} \beta^2 \mu}{7s^2} - \frac{5\sqrt{\frac{2}{3}} \beta^3 \mu^2 t}{21s^2} \\
 & - \frac{2\sqrt{\frac{2}{3}} \beta^3 \mu^2}{7s^2 t} - \frac{5\beta^3 t}{42\sqrt{6}s^2} - \frac{\beta^3}{7\sqrt{6}s^2 t} - \frac{\sqrt{\frac{3}{2}} \beta^2}{7s^2 t} \\
 & \left. + \frac{\beta t}{2\sqrt{6}s^2} - \frac{\sqrt{\frac{3}{2}} \beta^2 \mu^2}{7t} - \frac{\sqrt{\frac{3}{2}} \beta^2}{14t} - \frac{\beta}{2\sqrt{6}t} \right\}
 \end{aligned}
 \tag{B8}$$

$$\begin{aligned}
 [\bar{T}_{31}]_2^1 = & \sqrt{1-\mu^2} \left\{ -\frac{10\sqrt{\frac{2}{3}} \beta^4 \mu^4 t^5}{231s^4} - \frac{10\sqrt{\frac{2}{3}} \beta^4 \mu^2 t^5}{77s^4} \right. \\
 & - \frac{5\beta^4 t^5}{154\sqrt{6}s^4} - \frac{5\sqrt{\frac{2}{3}} \beta^3 \mu^2 t^5}{21s^4} - \frac{5\beta^3 t^5}{42\sqrt{6}s^4} \\
 & + \frac{20\sqrt{\frac{2}{3}} \beta^4 \mu^3 t^4}{77s^4} + \frac{5\sqrt{6} \beta^4 \mu t^4}{77s^4} + \frac{4\sqrt{\frac{2}{3}} \beta^3 \mu^3 t^4}{21s^4} \\
 & + \frac{2\sqrt{\frac{2}{3}} \beta^3 \mu t^4}{7s^4} - \frac{\sqrt{6} \beta^2 \mu t^4}{7s^4} - \frac{15\sqrt{\frac{3}{2}} \beta^4 \mu^2 t^3}{77s^4} \\
 & - \frac{5\sqrt{\frac{3}{2}} \beta^4 t^3}{154s^4} + \frac{3\sqrt{\frac{3}{2}} \beta^2 \mu^2 t^3}{7s^4} + \frac{3\sqrt{\frac{3}{2}} \beta^2 t^3}{14s^4} \\
 & + \frac{5\beta^4 \mu t^2}{33\sqrt{6}s^4} - \frac{5\sqrt{\frac{2}{3}} \beta^3 \mu t^2}{21s^4} - \frac{3\sqrt{\frac{3}{2}} \beta^2 \mu t^2}{7s^4} + \frac{5\beta^3 t}{42\sqrt{6}s^4} \\
 & + \frac{\sqrt{\frac{3}{2}} \beta^2 t}{14s^4} - \frac{2\sqrt{\frac{2}{3}} \beta^3 \mu^2 t^3}{7s^2} - \frac{\beta^3 t^3}{7\sqrt{6}s^2} - \frac{\sqrt{6} \beta^2 \mu^2 t^3}{7s^2} \\
 & - \frac{\sqrt{\frac{3}{2}} \beta^2 t^3}{7s^2} + \frac{5\beta^3 \mu t^2}{7\sqrt{6}s^2} + \frac{\sqrt{6} \beta^2 \mu t^2}{7s^2} - \frac{\beta \mu t^2}{\sqrt{6}s^2} \\
 & \left. - \frac{5\beta^3 t}{42\sqrt{6}s^2} + \frac{\beta t}{2\sqrt{6}s^2} - \frac{1}{14} \sqrt{\frac{3}{2}} \beta^2 t - \frac{\beta t}{2\sqrt{6}} \right\}
 \end{aligned}
 \tag{B9}$$

$$\begin{aligned}
 [\bar{T}_{12}]_2^2 = & \frac{4}{77} \sqrt{\frac{2}{3}} \beta^4 \mu^4 - \frac{1}{77} \sqrt{6} \beta^4 \mu^2 - \frac{1}{77} \sqrt{\frac{2}{3}} \beta^4 \\
 & + \frac{1}{7} \sqrt{\frac{2}{3}} \beta^3 \mu^4 - \frac{\beta^3 \mu^2}{14\sqrt{6}} - \frac{1}{14} \sqrt{\frac{3}{2}} \beta^3 + \frac{5\beta^2 \mu^2}{7\sqrt{6}} \\
 & - \frac{5\beta^2}{7\sqrt{6}} + \frac{\beta \mu^2}{2\sqrt{6}} - \frac{\beta}{2\sqrt{6}} - \frac{5}{231} \sqrt{\frac{2}{3}} \beta^4 \mu^5 t \\
 & - \frac{5\beta^4 \mu^3 t}{231\sqrt{6}} - \frac{5\beta^4 \mu^3}{154\sqrt{6}t} + \frac{5\beta^4 \mu t}{77\sqrt{6}} + \frac{5\beta^4 \mu}{154\sqrt{6}t} \\
 & - \frac{4}{21} \sqrt{\frac{2}{3}} \beta^3 \mu^3 t - \frac{\beta^3 \mu^3}{7\sqrt{6}t} + \frac{4}{21} \sqrt{\frac{2}{3}} \beta^3 \mu t + \frac{\beta^3 \mu}{7\sqrt{6}t} \\
 & - \frac{1}{7} \sqrt{\frac{3}{2}} \beta^2 \mu^3 t - \frac{\sqrt{\frac{3}{2}} \beta^2 \mu^3}{14t} + \frac{1}{7} \sqrt{\frac{3}{2}} \beta^2 \mu t + \frac{\sqrt{\frac{3}{2}} \beta^2 \mu}{14t}
 \end{aligned}
 \tag{B10}$$

$$\begin{aligned}
 [\bar{T}_{23}]_2^2 = & -\frac{2\sqrt{6}\beta^4\mu^4}{77s^4} + \frac{3\sqrt{\frac{3}{2}}\beta^4\mu^2}{77s^4} + \frac{\sqrt{\frac{3}{2}}\beta^4}{77s^4} - \frac{\beta^3\mu^2}{21\sqrt{6}s^4} \\
 & + \frac{\beta^3}{21\sqrt{6}s^4} - \frac{5\beta^3\mu^3t^3}{21\sqrt{6}s^4} + \frac{5\beta^3\mu t^3}{21\sqrt{6}s^4} - \frac{\sqrt{\frac{3}{2}}\beta^2\mu^3t^3}{14s^4} \\
 & + \frac{\sqrt{\frac{3}{2}}\beta^2\mu t^3}{14s^4} - \frac{5\sqrt{\frac{2}{3}}\beta^4\mu^4t^2}{77s^4} + \frac{5\sqrt{\frac{3}{2}}\beta^4\mu^2t^2}{154s^4} \\
 & + \frac{5\beta^4t^2}{154\sqrt{6}s^4} + \frac{2\sqrt{\frac{2}{3}}\beta^3\mu^4t^2}{21s^4} - \frac{\sqrt{\frac{2}{3}}\beta^3\mu^2t^2}{21s^4} \\
 & - \frac{\sqrt{\frac{2}{3}}\beta^3t^2}{21s^4} + \frac{\sqrt{\frac{3}{2}}\beta^2\mu^2t^2}{14s^4} - \frac{\sqrt{\frac{3}{2}}\beta^2t^2}{14s^4} \\
 & + \frac{5\sqrt{\frac{2}{3}}\beta^4\mu^5t}{77s^4} + \frac{5\beta^4\mu^3t}{77\sqrt{6}s^4} + \frac{5\beta^4\mu^3}{154\sqrt{6}s^4t} - \frac{5\sqrt{\frac{3}{2}}\beta^4\mu t}{77s^4} \\
 & - \frac{5\beta^4\mu}{154\sqrt{6}s^4t} - \frac{\sqrt{\frac{2}{3}}\beta^3\mu^4}{7s^2} + \frac{\beta^3\mu^2}{7\sqrt{6}s^2} + \frac{\beta^3}{7\sqrt{6}s^2} \\
 & - \frac{\beta^2\mu^2}{7\sqrt{6}s^2} + \frac{\beta^2}{7\sqrt{6}s^2} + \frac{5\beta^3\mu^3t}{21\sqrt{6}s^2} + \frac{\beta^3\mu^3}{7\sqrt{6}s^2t} \\
 & - \frac{5\beta^3\mu t}{21\sqrt{6}s^2} - \frac{\beta^3\mu}{7\sqrt{6}s^2t} + \frac{\sqrt{\frac{3}{2}}\beta^2\mu^3}{14t} - \frac{\sqrt{\frac{3}{2}}\beta^2\mu}{14t}
 \end{aligned} \tag{B11}$$

$$\begin{aligned}
 [\bar{T}_{31}]_2^2 = & \frac{5\sqrt{\frac{2}{3}}\beta^4\mu^5t^5}{231s^4} + \frac{5\beta^4\mu^3t^5}{231\sqrt{6}s^4} - \frac{5\beta^4\mu t^5}{77\sqrt{6}s^4} + \frac{5\beta^3\mu^3t^5}{21\sqrt{6}s^4} \\
 & - \frac{5\beta^3\mu t^5}{21\sqrt{6}s^4} - \frac{2\sqrt{6}\beta^4\mu^4t^4}{77s^4} + \frac{3\sqrt{\frac{3}{2}}\beta^4\mu^2t^4}{77s^4} + \frac{\sqrt{\frac{3}{2}}\beta^4t^4}{77s^4} \\
 & - \frac{2\sqrt{\frac{2}{3}}\beta^3\mu^4t^4}{21s^4} + \frac{\sqrt{\frac{2}{3}}\beta^3\mu^2t^4}{21s^4} + \frac{\sqrt{\frac{2}{3}}\beta^3t^4}{21s^4} \\
 & + \frac{\sqrt{\frac{3}{2}}\beta^2\mu^2t^4}{7s^4} - \frac{\sqrt{\frac{3}{2}}\beta^2t^4}{7s^4} + \frac{5\sqrt{\frac{3}{2}}\beta^4\mu^3t^3}{154s^4} \\
 & - \frac{5\sqrt{\frac{3}{2}}\beta^4\mu t^3}{154s^4} - \frac{3\sqrt{\frac{3}{2}}\beta^2\mu^3t^3}{14s^4} + \frac{3\sqrt{\frac{3}{2}}\beta^2\mu t^3}{14s^4} \\
 & - \frac{5\beta^4\mu^2t^2}{462\sqrt{6}s^4} + \frac{5\beta^4t^2}{462\sqrt{6}s^4} + \frac{\beta^3\mu^2t^2}{21\sqrt{6}s^4} - \frac{\beta^3t^2}{21\sqrt{6}s^4} \\
 & + \frac{\sqrt{\frac{3}{2}}\beta^2\mu^2t^2}{14s^4} - \frac{\sqrt{\frac{3}{2}}\beta^2t^2}{14s^4} + \frac{\beta^3\mu^3t^3}{7\sqrt{6}s^2} - \frac{\beta^3\mu t^3}{7\sqrt{6}s^2} \\
 & + \frac{\sqrt{\frac{3}{2}}\beta^2\mu^3t^3}{7s^2} - \frac{\sqrt{\frac{3}{2}}\beta^2\mu t^3}{7s^2} - \frac{\beta^3\mu^2t^2}{14\sqrt{6}s^2} + \frac{\beta^3t^2}{14\sqrt{6}s^2} \\
 & - \frac{\beta^2\mu^2t^2}{7\sqrt{6}s^2} + \frac{\beta^2t^2}{7\sqrt{6}s^2} + \frac{\beta\mu^2t^2}{2\sqrt{6}s^2} - \frac{\beta t^2}{2\sqrt{6}s^2}
 \end{aligned} \tag{B12}$$

$$\begin{aligned}
 [\bar{T}_{12}]_4^0 = & -\frac{1929\beta^4\mu^4}{5005} + \frac{138\beta^4\mu^2}{5005} + \frac{111\beta^4}{5005} \\
 & - \frac{117\beta^3\mu^4}{154} - \frac{123\beta^3\mu^2}{385} + \frac{111\beta^3}{770} - \frac{\beta^2\mu^4}{2} \\
 & - \frac{9\beta^2\mu^2}{35} + \frac{\beta^2}{14} + \frac{345\beta^4\mu^5t}{2002} + \frac{51\beta^4\mu^3t}{1001} \\
 & + \frac{186\beta^4\mu^3}{1001t} - \frac{111\beta^4\mu t}{2002} - \frac{18\beta^4\mu}{1001t} + \frac{5}{22}\beta^3\mu^5t \\
 & + \frac{193}{385}\beta^3\mu^3t + \frac{24\beta^3\mu^3}{55t} - \frac{201}{770}\beta^3\mu t + \frac{12\beta^3\mu}{385t} \\
 & + \frac{4}{7}\beta^2\mu^3t + \frac{2\beta^2\mu^3}{7t} - \frac{8}{35}\beta^2\mu t + \frac{2\beta^2\mu}{35t}
 \end{aligned} \tag{B13}$$

$$\begin{aligned}
 [\bar{T}_{23}]_4^0 = & \frac{5787\beta^4\mu^4}{10010s^4} - \frac{207\beta^4\mu^2}{5005s^4} - \frac{333\beta^4}{10010s^4} + \frac{136\beta^3\mu^2}{385s^4} \\
 & - \frac{16\beta^3}{385s^4} - \frac{4\beta^2}{35s^4} + \frac{5\beta^3\mu^5t^3}{22s^4} + \frac{5\beta^3\mu^3t^3}{77s^4} - \frac{3\beta^3\mu t^3}{22s^4} \\
 & + \frac{2\beta^2\mu^3t^3}{7s^4} - \frac{6\beta^2\mu t^3}{35s^4} + \frac{15\beta^4\mu^6t^2}{143s^4} + \frac{405\beta^4\mu^4t^2}{2002s^4} \\
 & - \frac{18\beta^4\mu^2t^2}{143s^4} - \frac{27\beta^4t^2}{2002s^4} - \frac{39\beta^3\mu^4t^2}{77s^4} + \frac{54\beta^3\mu^2t^2}{385s^4} \\
 & + \frac{3\beta^3t^2}{55s^4} - \frac{18\beta^2\mu^2t^2}{35s^4} + \frac{6\beta^2t^2}{35s^4} - \frac{1035\beta^4\mu^5t}{2002s^4} \\
 & - \frac{153\beta^4\mu^3t}{1001s^4} - \frac{186\beta^4\mu^3}{1001s^4t} + \frac{333\beta^4\mu t}{2002s^4} + \frac{18\beta^4\mu}{1001s^4t} \\
 & - \frac{12\beta^3\mu}{77s^4t} + \frac{12\beta^2\mu t}{35s^4} + \frac{117\beta^3\mu^4}{154s^2} - \frac{81\beta^3\mu^2}{385s^2} - \frac{9\beta^3}{110s^2} \\
 & + \frac{12\beta^2\mu^2}{35s^2} - \frac{4\beta^2}{35s^2} - \frac{5\beta^3\mu^5t}{22s^2} - \frac{5\beta^3\mu^3t}{77s^2} - \frac{24\beta^3\mu^3}{55s^2t} \\
 & + \frac{3\beta^3\mu t}{22s^2} + \frac{48\beta^3\mu}{385s^2t} - \frac{8\beta^2\mu}{35s^2t} - \frac{2\beta^2\mu^3}{7t} + \frac{6\beta^2\mu}{35t}
 \end{aligned} \tag{B14}$$

$$\begin{aligned}
 [\bar{T}_{31}]_4^0 = & -\frac{345\beta^4\mu^5t^5}{2002s^4} - \frac{51\beta^4\mu^3t^5}{1001s^4} + \frac{111\beta^4\mu t^5}{2002s^4} - \frac{5\beta^3\mu^5t^5}{22s^4} \\
 & - \frac{5\beta^3\mu^3t^5}{77s^4} + \frac{3\beta^3\mu t^5}{22s^4} + \frac{5787\beta^4\mu^4t^4}{10010s^4} - \frac{207\beta^4\mu^2t^4}{5005s^4} \\
 & - \frac{333\beta^4t^4}{10010s^4} + \frac{39\beta^3\mu^4t^4}{77s^4} - \frac{54\beta^3\mu^2t^4}{385s^4} - \frac{3\beta^3t^4}{55s^4} \\
 & - \frac{\beta^2\mu^4t^4}{2s^4} + \frac{3\beta^2\mu^2t^4}{7s^4} - \frac{3\beta^2t^4}{70s^4} - \frac{558\beta^4\mu^3t^3}{1001s^4} \\
 & + \frac{54\beta^4\mu t^3}{1001s^4} + \frac{6\beta^2\mu^3t^3}{7s^4} - \frac{18\beta^2\mu t^3}{35s^4} + \frac{174\beta^4\mu^2t^2}{1001s^4} \\
 & - \frac{6\beta^4t^2}{1001s^4} - \frac{136\beta^3\mu^2t^2}{385s^4} + \frac{16\beta^3t^2}{385s^4} - \frac{18\beta^2\mu^2t^2}{35s^4} \\
 & + \frac{6\beta^2t^2}{35s^4} + \frac{12\beta^3\mu t}{77s^4} + \frac{4\beta^2\mu t}{35s^4} - \frac{24\beta^3\mu^3t^3}{55s^2} + \frac{48\beta^3\mu t^3}{385s^2} \\
 & - \frac{4\beta^2\mu^3t^3}{7s^2} + \frac{12\beta^2\mu t^3}{35s^2} + \frac{204\beta^3\mu^2t^2}{385s^2} - \frac{24\beta^3t^2}{385s^2} \\
 & + \frac{12\beta^2\mu^2t^2}{35s^2} - \frac{4\beta^2t^2}{35s^2} - \frac{12\beta^3\mu t}{77s^2} - \frac{4}{35}\beta^2\mu t
 \end{aligned} \tag{B15}$$

$$\begin{aligned}
 [\bar{T}_{12}]_4^1 = \sqrt{1-\mu^2} \left\{ -\frac{138\sqrt{5}\beta^4\mu^3}{1001} - \frac{30\sqrt{5}\beta^4\mu}{1001} \right. \\
 - \frac{111\beta^3\mu^3}{77\sqrt{5}} - \frac{69\beta^3\mu}{77\sqrt{5}} - \frac{\beta^2\mu^3}{\sqrt{5}} - \frac{1}{7}\sqrt{5}\beta^2\mu \\
 + \frac{6}{91}\sqrt{5}\beta^4\mu^4t + \frac{81\sqrt{5}\beta^4\mu^2t}{2002} + \frac{237\sqrt{5}\beta^4\mu^2}{4004t} \\
 - \frac{3\sqrt{5}\beta^4t}{2002} + \frac{15\sqrt{5}\beta^4}{4004t} + \frac{1}{11}\sqrt{5}\beta^3\mu^4t \\
 + \frac{81\beta^3\mu^2t}{77\sqrt{5}} + \frac{117\beta^3\mu^2}{154\sqrt{5}t} - \frac{6\beta^3t}{77\sqrt{5}} + \frac{23\beta^3}{154\sqrt{5}t} \\
 \left. + \frac{3}{14}\sqrt{5}\beta^2\mu^2t + \frac{3\sqrt{5}\beta^2\mu^2}{28t} - \frac{\beta^2t}{14\sqrt{5}} + \frac{\sqrt{5}\beta^2}{28t} \right\} \quad (B16)
 \end{aligned}$$

$$\begin{aligned}
 [\bar{T}_{23}]_4^1 = \sqrt{1-\mu^2} \left\{ \frac{207\sqrt{5}\beta^4\mu^3}{1001s^4} + \frac{45\sqrt{5}\beta^4\mu}{1001s^4} + \frac{8\sqrt{5}\beta^3\mu}{77s^4} \right. \\
 + \frac{\sqrt{5}\beta^3\mu^4t^3}{11s^4} + \frac{9\sqrt{5}\beta^3\mu^2t^3}{154s^4} - \frac{3\sqrt{5}\beta^3t^3}{154s^4} + \frac{3\sqrt{5}\beta^2\mu^2t^3}{28s^4} \\
 - \frac{3\beta^2t^3}{28\sqrt{5}s^4} + \frac{6\sqrt{5}\beta^4\mu^5t^2}{143s^4} + \frac{93\sqrt{5}\beta^4\mu^3t^2}{1001s^4} - \frac{9\sqrt{5}\beta^4\mu t^2}{1001s^4} \\
 - \frac{74\beta^3\mu^3t^2}{77\sqrt{5}s^4} - \frac{6\beta^3\mu t^2}{77\sqrt{5}s^4} - \frac{6\beta^2\mu t^2}{7\sqrt{5}s^4} - \frac{18\sqrt{5}\beta^4\mu^4t}{91s^4} \\
 - \frac{243\sqrt{5}\beta^4\mu^2t}{2002s^4} - \frac{237\sqrt{5}\beta^4\mu^2}{4004s^4t} + \frac{9\sqrt{5}\beta^4t}{2002s^4} - \frac{15\sqrt{5}\beta^4}{4004s^4t} \\
 - \frac{2\sqrt{5}\beta^3}{77s^4t} + \frac{3\beta^2t}{7\sqrt{5}s^4} + \frac{111\beta^3\mu^3}{77\sqrt{5}s^2} + \frac{9\beta^3\mu}{77\sqrt{5}s^2} + \frac{4\beta^2\mu}{7\sqrt{5}s^2} \\
 - \frac{\sqrt{5}\beta^3\mu^4t}{11s^2} - \frac{9\sqrt{5}\beta^3\mu^2t}{154s^2} - \frac{117\beta^3\mu^2}{154\sqrt{5}s^2t} + \frac{3\sqrt{5}\beta^3t}{154s^2} \\
 \left. - \frac{3\beta^3}{154\sqrt{5}s^2t} - \frac{2\beta^2}{7\sqrt{5}s^2t} - \frac{3\sqrt{5}\beta^2\mu^2}{28t} + \frac{3\beta^2}{28\sqrt{5}t} \right\} \quad (B17)
 \end{aligned}$$

$$\begin{aligned}
 [\bar{T}_{31}]_4^1 = \sqrt{1-\mu^2} \left\{ -\frac{6\sqrt{5}\beta^4\mu^4t^5}{91s^4} - \frac{81\sqrt{5}\beta^4\mu^2t^5}{2002s^4} \right. \\
 + \frac{3\sqrt{5}\beta^4t^5}{2002s^4} - \frac{\sqrt{5}\beta^3\mu^4t^5}{11s^4} - \frac{9\sqrt{5}\beta^3\mu^2t^5}{154s^4} + \frac{3\sqrt{5}\beta^3t^5}{154s^4} \\
 + \frac{207\sqrt{5}\beta^4\mu^3t^4}{1001s^4} + \frac{45\sqrt{5}\beta^4\mu t^4}{1001s^4} + \frac{74\beta^3\mu^3t^4}{77\sqrt{5}s^4} \\
 + \frac{6\beta^3\mu t^4}{77\sqrt{5}s^4} - \frac{\beta^2\mu^3t^4}{\sqrt{5}s^4} + \frac{3\beta^2\mu t^4}{7\sqrt{5}s^4} - \frac{711\sqrt{5}\beta^4\mu^2t^3}{4004s^4} \\
 - \frac{45\sqrt{5}\beta^4t^3}{4004s^4} + \frac{9\sqrt{5}\beta^2\mu^2t^3}{28s^4} - \frac{9\beta^2t^3}{28\sqrt{5}s^4} + \frac{6\sqrt{5}\beta^4\mu t^2}{143s^4} \\
 - \frac{8\sqrt{5}\beta^3\mu t^2}{77s^4} - \frac{6\beta^2\mu t^2}{7\sqrt{5}s^4} + \frac{2\sqrt{5}\beta^3t}{77s^4} + \frac{\beta^2t}{7\sqrt{5}s^4} \\
 - \frac{117\beta^3\mu^2t^3}{154\sqrt{5}s^2} - \frac{3\beta^3t^3}{154\sqrt{5}s^2} - \frac{3\sqrt{5}\beta^2\mu^2t^3}{14s^2} + \frac{3\beta^2t^3}{14\sqrt{5}s^2} \\
 \left. + \frac{12\sqrt{5}\beta^3\mu t^2}{77s^2} + \frac{4\beta^2\mu t^2}{7\sqrt{5}s^2} - \frac{2\sqrt{5}\beta^3t}{77s^2} - \frac{\beta^2t}{7\sqrt{5}} \right\} \quad (B18)
 \end{aligned}$$

$$\begin{aligned}
 [\bar{T}_{12}]_4^2 = \frac{237\sqrt{\frac{2}{5}}\beta^4\mu^4}{1001} - \frac{204\sqrt{\frac{2}{5}}\beta^4\mu^2}{1001} - \frac{3}{91}\sqrt{\frac{2}{5}}\beta^4 + \frac{93\beta^3\mu^4}{77\sqrt{10}} \\
 - \frac{6}{77}\sqrt{10}\beta^3\mu^2 - \frac{3\beta^3}{7\sqrt{10}} + \frac{\beta^2\mu^4}{\sqrt{10}} - \frac{2}{7}\sqrt{\frac{2}{5}}\beta^2\mu^2 - \frac{3\beta^2}{7\sqrt{10}} \\
 - \frac{57\sqrt{\frac{5}{2}}\beta^4\mu^5t}{1001} + \frac{12\sqrt{10}\beta^4\mu^3t}{1001} - \frac{27\sqrt{\frac{5}{2}}\beta^4\mu^3}{1001t} \\
 + \frac{3}{91}\sqrt{\frac{5}{2}}\beta^4\mu t + \frac{27\sqrt{\frac{5}{2}}\beta^4\mu}{1001t} - \frac{1}{11}\sqrt{\frac{5}{2}}\beta^3\mu^5t \\
 - \frac{13}{77}\sqrt{\frac{2}{5}}\beta^3\mu^3t - \frac{18\sqrt{\frac{2}{5}}\beta^3\mu^3}{77t} + \frac{61\beta^3\mu t}{77\sqrt{10}} + \frac{18\sqrt{\frac{2}{5}}\beta^3\mu}{77t} \\
 - \frac{3}{7}\sqrt{\frac{2}{5}}\beta^2\mu^3t - \frac{3\beta^2\mu^3}{7\sqrt{10}t} + \frac{3}{7}\sqrt{\frac{2}{5}}\beta^2\mu t + \frac{3\beta^2\mu}{7\sqrt{10}t} \quad (B19)
 \end{aligned}$$

$$\begin{aligned}
 [\bar{T}_{23}]_4^2 = -\frac{711\beta^4\mu^4}{1001\sqrt{10}s^4} + \frac{306\sqrt{\frac{2}{5}}\beta^4\mu^2}{1001s^4} + \frac{9\beta^4}{91\sqrt{10}s^4} \\
 - \frac{6\sqrt{\frac{2}{5}}\beta^3\mu^2}{77s^4} + \frac{6\sqrt{\frac{2}{5}}\beta^3}{77s^4} - \frac{\sqrt{\frac{5}{2}}\beta^3\mu^5t^3}{11s^4} + \frac{\sqrt{10}\beta^3\mu^3t^3}{77s^4} \\
 + \frac{5\sqrt{\frac{5}{2}}\beta^3\mu t^3}{77s^4} - \frac{3\beta^2\mu^3t^3}{7\sqrt{10}s^4} + \frac{3\beta^2\mu t^3}{7\sqrt{10}s^4} - \frac{3\sqrt{10}\beta^4\mu^6t^2}{143s^4} \\
 - \frac{45\sqrt{\frac{5}{2}}\beta^4\mu^4t^2}{1001s^4} + \frac{81\sqrt{\frac{5}{2}}\beta^4\mu^2t^2}{1001s^4} + \frac{3\sqrt{10}\beta^4t^2}{1001s^4} \\
 + \frac{31\sqrt{\frac{2}{5}}\beta^3\mu^4t^2}{77s^4} - \frac{26\sqrt{\frac{2}{5}}\beta^3\mu^2t^2}{77s^4} - \frac{\sqrt{10}\beta^3t^2}{77s^4} \\
 + \frac{3\beta^2\mu^2t^2}{7\sqrt{10}s^4} - \frac{3\beta^2t^2}{7\sqrt{10}s^4} + \frac{171\sqrt{\frac{5}{2}}\beta^4\mu^5t}{1001s^4} - \frac{36\sqrt{10}\beta^4\mu^3t}{1001s^4} \\
 + \frac{27\sqrt{\frac{5}{2}}\beta^4\mu^3}{1001s^4t} - \frac{9\sqrt{\frac{5}{2}}\beta^4\mu t}{91s^4} - \frac{27\sqrt{\frac{5}{2}}\beta^4\mu}{1001s^4t} - \frac{93\beta^3\mu^4}{77\sqrt{10}s^2} \\
 + \frac{39\sqrt{\frac{2}{5}}\beta^3\mu^2}{77s^2} + \frac{3\sqrt{\frac{5}{2}}\beta^3}{77s^2} - \frac{\sqrt{\frac{2}{5}}\beta^2\mu^2}{7s^2} + \frac{\sqrt{\frac{2}{5}}\beta^2}{7s^2} \\
 + \frac{\sqrt{\frac{5}{2}}\beta^3\mu^5t}{11s^2} - \frac{\sqrt{10}\beta^3\mu^3t}{77s^2} + \frac{18\sqrt{\frac{2}{5}}\beta^3\mu^3}{77s^2t} \\
 - \frac{5\sqrt{\frac{5}{2}}\beta^3\mu t}{77s^2} - \frac{18\sqrt{\frac{2}{5}}\beta^3\mu}{77s^2t} + \frac{3\beta^2\mu^3}{7\sqrt{10}t} - \frac{3\beta^2\mu}{7\sqrt{10}t} \quad (B20)
 \end{aligned}$$

$$\begin{aligned}
[\bar{T}_{31}]_4^2 &= \frac{57\sqrt{\frac{5}{2}}\beta^4\mu^5t^5}{1001s^4} - \frac{12\sqrt{10}\beta^4\mu^3t^5}{1001s^4} - \frac{3\sqrt{\frac{5}{2}}\beta^4\mu t^5}{91s^4} \\
&+ \frac{\sqrt{\frac{5}{2}}\beta^3\mu^5t^5}{11s^4} - \frac{\sqrt{10}\beta^3\mu^3t^5}{77s^4} - \frac{5\sqrt{\frac{5}{2}}\beta^3\mu t^5}{77s^4} \\
&- \frac{711\beta^4\mu^4t^4}{1001\sqrt{10}s^4} + \frac{306\sqrt{\frac{2}{5}}\beta^4\mu^2t^4}{1001s^4} + \frac{9\beta^4t^4}{91\sqrt{10}s^4} \\
&- \frac{31\sqrt{\frac{2}{5}}\beta^3\mu^4t^4}{77s^4} + \frac{26\sqrt{\frac{2}{5}}\beta^3\mu^2t^4}{77s^4} + \frac{\sqrt{10}\beta^3t^4}{77s^4} \\
&+ \frac{\beta^2\mu^4t^4}{\sqrt{10}s^4} - \frac{4\sqrt{\frac{2}{5}}\beta^2\mu^2t^4}{7s^4} + \frac{\beta^2t^4}{7\sqrt{10}s^4} + \frac{81\sqrt{\frac{5}{2}}\beta^4\mu^3t^3}{1001s^4} \\
&- \frac{81\sqrt{\frac{5}{2}}\beta^4\mu t^3}{1001s^4} - \frac{9\beta^2\mu^3t^3}{7\sqrt{10}s^4} + \frac{9\beta^2\mu t^3}{7\sqrt{10}s^4} - \frac{9\sqrt{\frac{5}{2}}\beta^4\mu^2t^2}{1001s^4} \\
&+ \frac{9\sqrt{\frac{5}{2}}\beta^4t^2}{1001s^4} + \frac{6\sqrt{\frac{2}{5}}\beta^3\mu^2t^2}{77s^4} - \frac{6\sqrt{\frac{2}{5}}\beta^3t^2}{77s^4} + \frac{3\beta^2\mu^2t^2}{7\sqrt{10}s^4} \\
&- \frac{3\beta^2t^2}{7\sqrt{10}s^4} + \frac{18\sqrt{\frac{2}{5}}\beta^3\mu^3t^3}{77s^2} - \frac{18\sqrt{\frac{2}{5}}\beta^3\mu t^3}{77s^2} \\
&+ \frac{3\sqrt{\frac{2}{5}}\beta^2\mu^3t^3}{7s^2} - \frac{3\sqrt{\frac{2}{5}}\beta^2\mu t^3}{7s^2} - \frac{9\sqrt{\frac{2}{5}}\beta^3\mu^2t^2}{77s^2} \\
&+ \frac{9\sqrt{\frac{2}{5}}\beta^3t^2}{77s^2} - \frac{\sqrt{\frac{2}{5}}\beta^2\mu^2t^2}{7s^2} + \frac{\sqrt{\frac{2}{5}}\beta^2t^2}{7s^2}
\end{aligned} \tag{B21}$$

$$\begin{aligned}
[\bar{T}_{12}]_4^3 &= \sqrt{1-\mu^2} \left\{ \frac{6}{143} \sqrt{\frac{5}{7}}\beta^4\mu^3 - \frac{6}{143} \sqrt{\frac{5}{7}}\beta^4\mu \right. \\
&+ \frac{9\beta^3\mu^3}{11\sqrt{35}} - \frac{9\beta^3\mu}{11\sqrt{35}} + \frac{\beta^2\mu^3}{\sqrt{35}} - \frac{\beta^2\mu}{\sqrt{35}} \\
&- \frac{6}{143} \sqrt{\frac{5}{7}}\beta^4\mu^4t + \frac{9}{286} \sqrt{\frac{5}{7}}\beta^4\mu^2t - \frac{3\sqrt{\frac{5}{7}}\beta^4\mu^2}{572t} \\
&+ \frac{3}{286} \sqrt{\frac{5}{7}}\beta^4t + \frac{3\sqrt{\frac{5}{7}}\beta^4}{572t} - \frac{1}{11} \sqrt{\frac{5}{7}}\beta^3\mu^4t \\
&+ \frac{\beta^3\mu^2t}{11\sqrt{35}} - \frac{3\beta^3\mu^2}{22\sqrt{35}t} + \frac{4\beta^3t}{11\sqrt{35}} + \frac{3\beta^3}{22\sqrt{35}t} \\
&\left. - \frac{\beta^2\mu^2t}{2\sqrt{35}} - \frac{\beta^2\mu^2}{4\sqrt{35}t} + \frac{\beta^2t}{2\sqrt{35}} + \frac{\beta^2}{4\sqrt{35}t} \right\}
\end{aligned} \tag{B22}$$

$$\begin{aligned}
[\bar{T}_{23}]_4^3 &= \sqrt{1-\mu^2} \left\{ -\frac{9\sqrt{\frac{5}{7}}\beta^4\mu^3}{143s^4} + \frac{9\sqrt{\frac{5}{7}}\beta^4\mu}{143s^4} - \frac{\sqrt{\frac{5}{7}}\beta^3\mu^4t^3}{11s^4} \right. \\
&+ \frac{\sqrt{\frac{5}{7}}\beta^3\mu^2t^3}{22s^4} + \frac{\sqrt{\frac{5}{7}}\beta^3t^3}{22s^4} - \frac{\beta^2\mu^2t^3}{4\sqrt{35}s^4} \\
&+ \frac{\beta^2t^3}{4\sqrt{35}s^4} - \frac{6\sqrt{\frac{5}{7}}\beta^4\mu^5t^2}{143s^4} - \frac{3\sqrt{\frac{5}{7}}\beta^4\mu^3t^2}{143s^4} \\
&+ \frac{9\sqrt{\frac{5}{7}}\beta^4\mu t^2}{143s^4} + \frac{6\beta^3\mu^3t^2}{11\sqrt{35}s^4} - \frac{6\beta^3\mu t^2}{11\sqrt{35}s^4} \\
&+ \frac{18\sqrt{\frac{5}{7}}\beta^4\mu^4t}{143s^4} - \frac{27\sqrt{\frac{5}{7}}\beta^4\mu^2t}{286s^4} + \frac{3\sqrt{\frac{5}{7}}\beta^4\mu^2}{572s^4t} \\
&- \frac{9\sqrt{\frac{5}{7}}\beta^4t}{286s^4} - \frac{3\sqrt{\frac{5}{7}}\beta^4}{572s^4t} - \frac{9\beta^3\mu^3}{11\sqrt{35}s^2} + \frac{9\beta^3\mu}{11\sqrt{35}s^2} \\
&+ \frac{\sqrt{\frac{5}{7}}\beta^3\mu^4t}{11s^2} - \frac{\sqrt{\frac{5}{7}}\beta^3\mu^2t}{22s^2} + \frac{3\beta^3\mu^2}{22\sqrt{35}s^2t} \\
&\left. - \frac{\sqrt{\frac{5}{7}}\beta^3t}{22s^2} - \frac{3\beta^3}{22\sqrt{35}s^2t} + \frac{\beta^2\mu^2}{4\sqrt{35}t} - \frac{\beta^2}{4\sqrt{35}t} \right\}
\end{aligned} \tag{B23}$$

$$\begin{aligned}
[\bar{T}_{31}]_4^3 &= \sqrt{1-\mu^2} \left\{ \frac{6\sqrt{\frac{5}{7}}\beta^4\mu^4t^5}{143s^4} - \frac{9\sqrt{\frac{5}{7}}\beta^4\mu^2t^5}{286s^4} \right. \\
&- \frac{3\sqrt{\frac{5}{7}}\beta^4t^5}{286s^4} + \frac{\sqrt{\frac{5}{7}}\beta^3\mu^4t^5}{11s^4} - \frac{\sqrt{\frac{5}{7}}\beta^3\mu^2t^5}{22s^4} \\
&- \frac{\sqrt{\frac{5}{7}}\beta^3t^5}{22s^4} - \frac{9\sqrt{\frac{5}{7}}\beta^4\mu^3t^4}{143s^4} + \frac{9\sqrt{\frac{5}{7}}\beta^4\mu t^4}{143s^4} \\
&- \frac{6\beta^3\mu^3t^4}{11\sqrt{35}s^4} + \frac{6\beta^3\mu t^4}{11\sqrt{35}s^4} + \frac{\beta^2\mu^3t^4}{\sqrt{35}s^4} - \frac{\beta^2\mu t^4}{\sqrt{35}s^4} \\
&+ \frac{9\sqrt{\frac{5}{7}}\beta^4\mu^2t^3}{572s^4} - \frac{9\sqrt{\frac{5}{7}}\beta^4t^3}{572s^4} - \frac{3\beta^2\mu^2t^3}{4\sqrt{35}s^4} + \frac{3\beta^2t^3}{4\sqrt{35}s^4} \\
&\left. + \frac{3\beta^3\mu^2t^3}{22\sqrt{35}s^2} - \frac{3\beta^3t^3}{22\sqrt{35}s^2} + \frac{\beta^2\mu^2t^3}{2\sqrt{35}s^2} - \frac{\beta^2t^3}{2\sqrt{35}s^2} \right\}
\end{aligned} \tag{B24}$$

$$\begin{aligned}
[\bar{T}_{12}]_4^4 &= -\frac{3\beta^4\mu^4}{143\sqrt{70}} + \frac{3}{143} \sqrt{\frac{2}{35}}\beta^4\mu^2 - \frac{3\beta^4}{143\sqrt{70}} - \frac{3\beta^3\mu^4}{22\sqrt{70}} \\
&+ \frac{3\beta^3\mu^2}{11\sqrt{70}} - \frac{3\beta^3}{22\sqrt{70}} - \frac{\beta^2\mu^4}{2\sqrt{70}} + \frac{\beta^2\mu^2}{\sqrt{70}} - \frac{\beta^2}{2\sqrt{70}} \\
&+ \frac{3}{286} \sqrt{\frac{5}{14}}\beta^4\mu^5t - \frac{3}{143} \sqrt{\frac{5}{14}}\beta^4\mu^3t + \frac{3}{286} \sqrt{\frac{5}{14}}\beta^4\mu t \\
&+ \frac{1}{22} \sqrt{\frac{5}{14}}\beta^3\mu^5t - \frac{1}{11} \sqrt{\frac{5}{14}}\beta^3\mu^3t + \frac{1}{22} \sqrt{\frac{5}{14}}\beta^3\mu t
\end{aligned} \tag{B25}$$



$$\begin{aligned}
 [\bar{T}_{23}]_4^4 = & \frac{9\beta^4\mu^4}{286\sqrt{70}s^4} - \frac{9\beta^4\mu^2}{143\sqrt{70}s^4} + \frac{9\beta^4}{286\sqrt{70}s^4} + \frac{\sqrt{\frac{5}{14}}\beta^3\mu^5t^3}{22s^4} \\
 & - \frac{\sqrt{\frac{5}{14}}\beta^3\mu^3t^3}{11s^4} + \frac{\sqrt{\frac{5}{14}}\beta^3\mu t^3}{22s^4} + \frac{3\sqrt{\frac{5}{14}}\beta^4\mu^6t^2}{143s^4} \\
 & - \frac{9\sqrt{\frac{5}{14}}\beta^4\mu^4t^2}{286s^4} + \frac{3\sqrt{\frac{5}{14}}\beta^4t^2}{286s^4} - \frac{\beta^3\mu^4t^2}{11\sqrt{70}s^4} \\
 & + \frac{\sqrt{\frac{2}{35}}\beta^3\mu^2t^2}{11s^4} - \frac{\beta^3t^2}{11\sqrt{70}s^4} - \frac{9\sqrt{\frac{5}{14}}\beta^4\mu^5t}{286s^4} \\
 & + \frac{9\sqrt{\frac{5}{14}}\beta^4\mu^3t}{143s^4} - \frac{9\sqrt{\frac{5}{14}}\beta^4\mu t}{286s^4} + \frac{3\beta^3\mu^4}{22\sqrt{70}s^2} - \frac{3\beta^3\mu^2}{11\sqrt{70}s^2} \\
 & + \frac{3\beta^3}{22\sqrt{70}s^2} - \frac{\sqrt{\frac{5}{14}}\beta^3\mu^5t}{22s^2} + \frac{\sqrt{\frac{5}{14}}\beta^3\mu^3t}{11s^2} - \frac{\sqrt{\frac{5}{14}}\beta^3\mu t}{22s^2}
 \end{aligned} \tag{B26}$$

$$\begin{aligned}
 [\bar{T}_{31}]_4^4 = & -\frac{3\sqrt{\frac{5}{14}}\beta^4\mu^5t^5}{286s^4} + \frac{3\sqrt{\frac{5}{14}}\beta^4\mu^3t^5}{143s^4} - \frac{3\sqrt{\frac{5}{14}}\beta^4\mu t^5}{286s^4} \\
 & - \frac{\sqrt{\frac{5}{14}}\beta^3\mu^5t^5}{22s^4} + \frac{\sqrt{\frac{5}{14}}\beta^3\mu^3t^5}{11s^4} - \frac{\sqrt{\frac{5}{14}}\beta^3\mu t^5}{22s^4} \\
 & + \frac{9\beta^4\mu^4t^4}{286\sqrt{70}s^4} - \frac{9\beta^4\mu^2t^4}{143\sqrt{70}s^4} + \frac{9\beta^4t^4}{286\sqrt{70}s^4} \\
 & + \frac{\beta^3\mu^4t^4}{11\sqrt{70}s^4} - \frac{\sqrt{\frac{2}{35}}\beta^3\mu^2t^4}{11s^4} + \frac{\beta^3t^4}{11\sqrt{70}s^4} \\
 & - \frac{\beta^2\mu^4t^4}{2\sqrt{70}s^4} + \frac{\beta^2\mu^2t^4}{\sqrt{70}s^4} - \frac{\beta^2t^4}{2\sqrt{70}s^4}
 \end{aligned} \tag{B27}$$

$$\begin{aligned}
 [\bar{T}_{12}]_6^0 = & -\frac{212\beta^4\mu^4}{693} + \frac{40\beta^4\mu^2}{231} + \frac{4\beta^4}{1155} - \frac{5\beta^3\mu^4}{11} \\
 & + \frac{18\beta^3\mu^2}{77} + \frac{\beta^3}{77} + \frac{34}{165}\beta^4\mu^5t - \frac{92}{693}\beta^4\mu^3t \\
 & + \frac{76\beta^4\mu^3}{693t} - \frac{2}{231}\beta^4\mu t - \frac{52\beta^4\mu}{1155t} + \frac{3}{11}\beta^3\mu^5t \\
 & - \frac{10}{77}\beta^3\mu^3t + \frac{40\beta^3\mu^3}{231t} - \frac{3}{77}\beta^3\mu t - \frac{16\beta^3\mu}{231t}
 \end{aligned} \tag{B28}$$

$$\begin{aligned}
 [\bar{T}_{23}]_6^0 = & \frac{106\beta^4\mu^4}{231s^4} - \frac{20\beta^4\mu^2}{77s^4} - \frac{2\beta^4}{385s^4} + \frac{8\beta^3\mu^2}{77s^4} - \frac{8\beta^3}{231s^4} \\
 & + \frac{3\beta^3\mu^5t^3}{11s^4} - \frac{10\beta^3\mu^3t^3}{33s^4} + \frac{5\beta^3\mu t^3}{77s^4} + \frac{83\beta^4\mu^6t^2}{330s^4} \\
 & - \frac{3\beta^4\mu^4t^2}{22s^4} - \frac{29\beta^4\mu^2t^2}{462s^4} + \frac{17\beta^4t^2}{1386s^4} - \frac{10\beta^3\mu^4t^2}{33s^4} \\
 & + \frac{20\beta^3\mu^2t^2}{77s^4} - \frac{2\beta^3t^2}{77s^4} - \frac{34\beta^4\mu^5t}{55s^4} + \frac{92\beta^4\mu^3t}{231s^4} \\
 & - \frac{76\beta^4\mu^3}{693s^4t} + \frac{2\beta^4\mu t}{77s^4} + \frac{52\beta^4\mu}{1155s^4t} - \frac{8\beta^3\mu}{231s^4t} \\
 & + \frac{5\beta^3\mu^4}{11s^2} - \frac{30\beta^3\mu^2}{77s^2} + \frac{3\beta^3}{77s^2} - \frac{3\beta^3\mu^5t}{11s^2} \\
 & + \frac{10\beta^3\mu^3t}{33s^2} - \frac{40\beta^3\mu^3}{231s^2t} - \frac{5\beta^3\mu t}{77s^2} + \frac{8\beta^3\mu}{77s^2t}
 \end{aligned} \tag{B29}$$

$$\begin{aligned}
 [\bar{T}_{31}]_6^0 = & -\frac{34\beta^4\mu^5t^5}{165s^4} + \frac{92\beta^4\mu^3t^5}{693s^4} + \frac{2\beta^4\mu t^5}{231s^4} - \frac{3\beta^3\mu^5t^5}{11s^4} \\
 & + \frac{10\beta^3\mu^3t^5}{33s^4} - \frac{5\beta^3\mu t^5}{77s^4} + \frac{106\beta^4\mu^4t^4}{231s^4} - \frac{20\beta^4\mu^2t^4}{77s^4} \\
 & - \frac{2\beta^4t^4}{385s^4} + \frac{10\beta^3\mu^4t^4}{33s^4} - \frac{20\beta^3\mu^2t^4}{77s^4} + \frac{2\beta^3t^4}{77s^4} \\
 & - \frac{76\beta^4\mu^3t^3}{231s^4} + \frac{52\beta^4\mu t^3}{385s^4} + \frac{92\beta^4\mu^2t^2}{1155s^4} - \frac{52\beta^4t^2}{3465s^4} \\
 & - \frac{8\beta^3\mu^2t^2}{77s^4} + \frac{8\beta^3t^2}{231s^4} + \frac{8\beta^3\mu t}{231s^4} - \frac{40\beta^3\mu^3t^3}{231s^2} \\
 & + \frac{8\beta^3\mu t^3}{77s^2} + \frac{12\beta^3\mu^2t^2}{77s^2} - \frac{4\beta^3t^2}{77s^2} - \frac{8\beta^3\mu t}{231s^2}
 \end{aligned} \tag{B30}$$

$$\begin{aligned}
 [\bar{T}_{12}]_6^1 = & \sqrt{1-\mu^2} \left\{ -\frac{136}{165}\sqrt{\frac{2}{21}}\beta^4\mu^3 + \frac{8}{55}\sqrt{\frac{2}{21}}\beta^4\mu \right. \\
 & - \frac{2}{11}\sqrt{\frac{14}{3}}\beta^3\mu^3 + \frac{2}{11}\sqrt{\frac{2}{21}}\beta^3\mu + \frac{1}{6}\sqrt{\frac{7}{6}}\beta^4\mu^4t \\
 & - \frac{1}{11}\sqrt{\frac{3}{14}}\beta^4\mu^2t + \frac{\sqrt{\frac{6}{7}}\beta^4\mu^2}{11t} - \frac{\beta^4t}{22\sqrt{42}} \\
 & - \frac{\sqrt{\frac{2}{21}}\beta^4}{55t} + \frac{5}{22}\sqrt{\frac{7}{6}}\beta^3\mu^4t - \frac{5\beta^3\mu^2t}{33\sqrt{42}} \\
 & \left. + \frac{5\sqrt{\frac{2}{21}}\beta^3\mu^2}{11t} - \frac{1}{66}\sqrt{\frac{7}{6}}\beta^3t - \frac{\sqrt{\frac{2}{21}}\beta^3}{33t} \right\}
 \end{aligned} \tag{B31}$$

$$\begin{aligned}
 [\bar{T}_{23}]_6^1 = & \sqrt{1-\mu^2} \left\{ \frac{68\sqrt{\frac{2}{21}}\beta^4\mu^3}{55s^4} - \frac{4\sqrt{\frac{6}{7}}\beta^4\mu}{55s^4} + \frac{8\sqrt{\frac{2}{21}}\beta^3\mu}{33s^4} \right. \\
 & + \frac{5\sqrt{\frac{7}{6}}\beta^3\mu^4t^3}{22s^4} - \frac{5\sqrt{\frac{7}{6}}\beta^3\mu^2t^3}{33s^4} + \frac{5\beta^3t^3}{66\sqrt{42}s^4} \\
 & + \frac{27\sqrt{\frac{3}{14}}\beta^4\mu^5t^2}{55s^4} - \frac{\sqrt{\frac{2}{21}}\beta^4\mu^3t^2}{11s^4} - \frac{\sqrt{\frac{3}{14}}\beta^4\mu t^2}{11s^4} \\
 & - \frac{4\sqrt{\frac{14}{3}}\beta^3\mu^3t^2}{33s^4} + \frac{4\sqrt{\frac{2}{21}}\beta^3\mu t^2}{11s^4} - \frac{\sqrt{\frac{7}{6}}\beta^4\mu^4t}{2s^4} \\
 & + \frac{3\sqrt{\frac{3}{14}}\beta^4\mu^2t}{11s^4} - \frac{\sqrt{\frac{6}{7}}\beta^4\mu^2}{11s^4t} + \frac{\sqrt{\frac{3}{14}}\beta^4t}{22s^4} + \frac{\sqrt{\frac{2}{21}}\beta^4}{55s^4t} \\
 & - \frac{2\sqrt{\frac{2}{21}}\beta^3}{33s^4t} + \frac{2\sqrt{\frac{14}{3}}\beta^3\mu^3}{11s^2} - \frac{2\sqrt{\frac{6}{7}}\beta^3\mu}{11s^2} - \frac{5\sqrt{\frac{7}{6}}\beta^3\mu^4t}{22s^2} \\
 & \left. + \frac{5\sqrt{\frac{7}{6}}\beta^3\mu^2t}{33s^2} - \frac{5\sqrt{\frac{2}{21}}\beta^3\mu^2}{11s^2t} - \frac{5\beta^3t}{66\sqrt{42}s^2} + \frac{\sqrt{\frac{2}{21}}\beta^3}{11s^2t} \right\}
 \end{aligned} \tag{B32}$$

$$\begin{aligned}
[\bar{T}_{31}]_6^1 &= \sqrt{1-\mu^2} \left\{ -\frac{\sqrt{\frac{7}{6}}\beta^4\mu^4t^5}{6s^4} + \frac{\sqrt{\frac{3}{14}}\beta^4\mu^2t^5}{11s^4} \right. \\
&+ \frac{\beta^4t^5}{22\sqrt{42}s^4} - \frac{5\sqrt{\frac{7}{6}}\beta^3\mu^4t^5}{22s^4} + \frac{5\sqrt{\frac{7}{6}}\beta^3\mu^2t^5}{33s^4} \\
&- \frac{5\beta^3t^5}{66\sqrt{42}s^4} + \frac{68\sqrt{\frac{2}{21}}\beta^4\mu^3t^4}{55s^4} - \frac{4\sqrt{\frac{6}{7}}\beta^4\mu^4t^4}{55s^4} \\
&+ \frac{4\sqrt{\frac{14}{3}}\beta^3\mu^3t^4}{33s^4} - \frac{4\sqrt{\frac{2}{21}}\beta^3\mu^4t^4}{11s^4} - \frac{3\sqrt{\frac{6}{7}}\beta^4\mu^2t^3}{11s^4} \\
&+ \frac{\sqrt{\frac{6}{7}}\beta^4t^3}{55s^4} + \frac{4\sqrt{\frac{14}{3}}\beta^4\mu t^2}{165s^4} - \frac{8\sqrt{\frac{2}{21}}\beta^3\mu t^2}{33s^4} \\
&+ \frac{2\sqrt{\frac{2}{21}}\beta^3t}{33s^4} - \frac{5\sqrt{\frac{2}{21}}\beta^3\mu^2t^3}{11s^2} + \frac{\sqrt{\frac{2}{21}}\beta^3t^3}{11s^2} \\
&\left. + \frac{4\sqrt{\frac{2}{21}}\beta^3\mu t^2}{11s^2} - \frac{2\sqrt{\frac{2}{21}}\beta^3t}{33s^2} \right\}
\end{aligned} \tag{B33}$$

$$\begin{aligned}
[\bar{T}_{12}]_6^2 &= \frac{16\beta^4\mu^4}{11\sqrt{105}} - \frac{16\beta^4\mu^2}{11\sqrt{105}} + \frac{4}{11}\sqrt{\frac{7}{15}}\beta^3\mu^4 \\
&- \frac{4}{11}\sqrt{\frac{7}{15}}\beta^3\mu^2 - \frac{8}{33}\sqrt{\frac{5}{21}}\beta^4\mu^5t + \frac{8}{33}\sqrt{\frac{5}{21}}\beta^4\mu^3t \\
&- \frac{4\beta^4\mu^3}{11\sqrt{105}t} + \frac{4\beta^4\mu}{11\sqrt{105}t} - \frac{4}{11}\sqrt{\frac{5}{21}}\beta^3\mu^5t \\
&+ \frac{8}{33}\sqrt{\frac{7}{15}}\beta^3\mu^3t - \frac{8\beta^3\mu^3}{11\sqrt{105}t} + \frac{4\beta^3\mu t}{33\sqrt{105}} + \frac{8\beta^3\mu}{11\sqrt{105}t}
\end{aligned} \tag{B34}$$

$$\begin{aligned}
[\bar{T}_{23}]_6^2 &= -\frac{8\sqrt{\frac{3}{35}}\beta^4\mu^4}{11s^4} + \frac{8\sqrt{\frac{3}{35}}\beta^4\mu^2}{11s^4} - \frac{8\beta^3\mu^2}{33\sqrt{105}s^4} \\
&+ \frac{8\beta^3}{33\sqrt{105}s^4} - \frac{4\sqrt{\frac{5}{21}}\beta^3\mu^5t^3}{11s^4} + \frac{16\sqrt{\frac{5}{21}}\beta^3\mu^3t^3}{33s^4} \\
&- \frac{4\sqrt{\frac{5}{21}}\beta^3\mu t^3}{33s^4} - \frac{5\sqrt{\frac{15}{7}}\beta^4\mu^6t^2}{44s^4} + \frac{13\sqrt{\frac{5}{21}}\beta^4\mu^4t^2}{44s^4} \\
&+ \frac{\sqrt{\frac{15}{7}}\beta^4\mu^2t^2}{44s^4} - \frac{\sqrt{\frac{5}{21}}\beta^4t^2}{44s^4} + \frac{8\sqrt{\frac{7}{15}}\beta^3\mu^4t^2}{33s^4} \\
&- \frac{64\beta^3\mu^2t^2}{33\sqrt{105}s^4} + \frac{8\beta^3t^2}{33\sqrt{105}s^4} + \frac{8\sqrt{\frac{5}{21}}\beta^4\mu^5t}{11s^4} \\
&- \frac{8\sqrt{\frac{5}{21}}\beta^4\mu^3t}{11s^4} + \frac{4\beta^4\mu^3}{11\sqrt{105}s^4t} - \frac{4\beta^4\mu}{11\sqrt{105}s^4t} \\
&- \frac{4\sqrt{\frac{7}{15}}\beta^3\mu^4}{11s^2} + \frac{32\beta^3\mu^2}{11\sqrt{105}s^2} - \frac{4\beta^3}{11\sqrt{105}s^2} \\
&+ \frac{4\sqrt{\frac{5}{21}}\beta^3\mu^5t}{11s^2} - \frac{16\sqrt{\frac{5}{21}}\beta^3\mu^3t}{33s^2} \\
&+ \frac{8\beta^3\mu^3}{11\sqrt{105}s^2t} + \frac{4\sqrt{\frac{5}{21}}\beta^3\mu t}{33s^2} - \frac{8\beta^3\mu}{11\sqrt{105}s^2t}
\end{aligned} \tag{B35}$$

$$\begin{aligned}
[\bar{T}_{31}]_6^2 &= \frac{8\sqrt{\frac{5}{21}}\beta^4\mu^5t^5}{33s^4} - \frac{8\sqrt{\frac{5}{21}}\beta^4\mu^3t^5}{33s^4} + \frac{4\sqrt{\frac{5}{21}}\beta^3\mu^5t^5}{11s^4} \\
&- \frac{16\sqrt{\frac{5}{21}}\beta^3\mu^3t^5}{33s^4} + \frac{4\sqrt{\frac{5}{21}}\beta^3\mu t^5}{33s^4} - \frac{8\sqrt{\frac{3}{35}}\beta^4\mu^4t^4}{11s^4} \\
&+ \frac{8\sqrt{\frac{3}{35}}\beta^4\mu^2t^4}{11s^4} - \frac{8\sqrt{\frac{7}{15}}\beta^3\mu^4t^4}{33s^4} + \frac{64\beta^3\mu^2t^4}{33\sqrt{105}s^4} \\
&- \frac{8\beta^3t^4}{33\sqrt{105}s^4} + \frac{4\sqrt{\frac{3}{35}}\beta^4\mu^3t^3}{11s^4} - \frac{4\sqrt{\frac{3}{35}}\beta^4\mu t^3}{11s^4} \\
&- \frac{4\beta^4\mu^2t^2}{33\sqrt{105}s^4} + \frac{4\beta^4t^2}{33\sqrt{105}s^4} + \frac{8\beta^3\mu^2t^2}{33\sqrt{105}s^4} - \frac{8\beta^3t^2}{33\sqrt{105}s^4} \\
&+ \frac{8\beta^3\mu^3t^3}{11\sqrt{105}s^2} - \frac{8\beta^3\mu t^3}{11\sqrt{105}s^2} - \frac{4\beta^3\mu^2t^2}{11\sqrt{105}s^2} + \frac{4\beta^3t^2}{11\sqrt{105}s^2}
\end{aligned} \tag{B36}$$

$$\begin{aligned}
[\bar{T}_{12}]_6^3 &= \sqrt{1-\mu^2} \left\{ \frac{16\beta^4\mu^3}{33\sqrt{105}} - \frac{16\beta^4\mu}{33\sqrt{105}} + \frac{4}{11}\sqrt{\frac{3}{35}}\beta^3\mu^3 \right. \\
&- \frac{4}{11}\sqrt{\frac{3}{35}}\beta^3\mu - \frac{5}{44}\sqrt{\frac{5}{21}}\beta^4\mu^4t + \frac{1}{66}\sqrt{\frac{35}{3}}\beta^4\mu^2t \\
&- \frac{2\beta^4\mu^2}{33\sqrt{105}t} + \frac{1}{132}\sqrt{\frac{5}{21}}\beta^4t + \frac{2\beta^4}{33\sqrt{105}t} \\
&- \frac{3}{44}\sqrt{\frac{15}{7}}\beta^3\mu^4t + \frac{1}{22}\sqrt{\frac{21}{5}}\beta^3\mu^2t \\
&\left. - \frac{2\beta^3\mu^2}{11\sqrt{105}t} + \frac{1}{44}\sqrt{\frac{3}{35}}\beta^3t + \frac{2\beta^3}{11\sqrt{105}t} \right\}
\end{aligned} \tag{B37}$$

$$\begin{aligned}
[\bar{T}_{23}]_6^3 &= \sqrt{1-\mu^2} \left\{ -\frac{8\beta^4\mu^3}{11\sqrt{105}s^4} + \frac{8\beta^4\mu}{11\sqrt{105}s^4} - \frac{3\sqrt{\frac{15}{7}}\beta^3\mu^4t^3}{44s^4} \right. \\
&+ \frac{5\sqrt{\frac{5}{21}}\beta^3\mu^2t^3}{22s^4} - \frac{\sqrt{\frac{5}{21}}\beta^3t^3}{44s^4} - \frac{13\sqrt{\frac{5}{21}}\beta^4\mu^5t^2}{66s^4} \\
&+ \frac{5\sqrt{\frac{5}{21}}\beta^4\mu^3t^2}{33s^4} + \frac{\sqrt{\frac{5}{21}}\beta^4\mu t^2}{22s^4} + \frac{8\beta^3\mu^3t^2}{11\sqrt{105}s^4} \\
&- \frac{8\beta^3\mu t^2}{11\sqrt{105}s^4} + \frac{5\sqrt{\frac{15}{7}}\beta^4\mu^4t}{44s^4} - \frac{\sqrt{\frac{35}{3}}\beta^4\mu^2t}{22s^4} \\
&+ \frac{2\beta^4\mu^2}{33\sqrt{105}s^4t} - \frac{\sqrt{\frac{5}{21}}\beta^4t}{44s^4} - \frac{2\beta^4}{33\sqrt{105}s^4t} - \frac{4\sqrt{\frac{3}{35}}\beta^3\mu^3}{11s^2} \\
&+ \frac{4\sqrt{\frac{3}{35}}\beta^3\mu}{11s^2} + \frac{3\sqrt{\frac{15}{7}}\beta^3\mu^4t}{44s^2} - \frac{5\sqrt{\frac{5}{21}}\beta^3\mu^2t}{22s^2} \\
&\left. + \frac{2\beta^3\mu^2}{11\sqrt{105}s^2t} + \frac{\sqrt{\frac{5}{21}}\beta^3t}{44s^2} - \frac{2\beta^3}{11\sqrt{105}s^2t} \right\}
\end{aligned} \tag{B38}$$

$$\begin{aligned}
 [\bar{T}_{31}]_6^3 = & \sqrt{1-\mu^2} \left\{ \frac{5\sqrt{\frac{5}{21}}\beta^4\mu^4t^5}{44s^4} - \frac{\sqrt{\frac{35}{3}}\beta^4\mu^2t^5}{66s^4} - \frac{\sqrt{\frac{5}{21}}\beta^4t^5}{132s^4} \right. \\
 & + \frac{3\sqrt{\frac{15}{7}}\beta^3\mu^4t^5}{44s^4} - \frac{5\sqrt{\frac{5}{21}}\beta^3\mu^2t^5}{22s^4} + \frac{\sqrt{\frac{5}{21}}\beta^3t^5}{44s^4} \\
 & - \frac{8\beta^4\mu^3t^4}{11\sqrt{105}s^4} + \frac{8\beta^4\mu t^4}{11\sqrt{105}s^4} - \frac{8\beta^3\mu^3t^4}{11\sqrt{105}s^4} + \frac{8\beta^3\mu t^4}{11\sqrt{105}s^4} \\
 & \left. + \frac{2\beta^4\mu^2t^3}{11\sqrt{105}s^4} - \frac{2\beta^4t^3}{11\sqrt{105}s^4} + \frac{2\beta^3\mu^2t^3}{11\sqrt{105}s^2} - \frac{2\beta^3t^3}{11\sqrt{105}s^2} \right\}
 \end{aligned} \tag{B39}$$

$$\begin{aligned}
 [\bar{T}_{12}]_6^4 = & -\frac{2}{165}\sqrt{\frac{2}{7}}\beta^4\mu^4 + \frac{4}{165}\sqrt{\frac{2}{7}}\beta^4\mu^2 - \frac{2}{165}\sqrt{\frac{2}{7}}\beta^4 \\
 & - \frac{\beta^3\mu^4}{11\sqrt{14}} + \frac{1}{11}\sqrt{\frac{2}{7}}\beta^3\mu^2 - \frac{\beta^3}{11\sqrt{14}} \\
 & + \frac{1}{33}\sqrt{\frac{2}{7}}\beta^4\mu^5t - \frac{2}{33}\sqrt{\frac{2}{7}}\beta^4\mu^3t + \frac{1}{33}\sqrt{\frac{2}{7}}\beta^4\mu t \\
 & + \frac{5\beta^3\mu^5t}{33\sqrt{14}} - \frac{5}{33}\sqrt{\frac{2}{7}}\beta^3\mu^3t + \frac{5\beta^3\mu t}{33\sqrt{14}}
 \end{aligned} \tag{B40}$$

$$\begin{aligned}
 [\bar{T}_{23}]_6^4 = & \frac{\sqrt{\frac{2}{7}}\beta^4\mu^4}{55s^4} - \frac{2\sqrt{\frac{2}{7}}\beta^4\mu^2}{55s^4} + \frac{\sqrt{\frac{2}{7}}\beta^4}{55s^4} + \frac{5\beta^3\mu^5t^3}{33\sqrt{14}s^4} \\
 & - \frac{5\sqrt{\frac{2}{7}}\beta^3\mu^3t^3}{33s^4} + \frac{5\beta^3\mu t^3}{33\sqrt{14}s^4} + \frac{17\beta^4\mu^6t^2}{110\sqrt{14}s^4} \\
 & - \frac{31\beta^4\mu^4t^2}{110\sqrt{14}s^4} + \frac{\beta^4\mu^2t^2}{10\sqrt{14}s^4} + \frac{3\beta^4t^2}{110\sqrt{14}s^4} - \frac{\sqrt{\frac{2}{7}}\beta^3\mu^4t^2}{33s^4} \\
 & + \frac{2\sqrt{\frac{2}{7}}\beta^3\mu^2t^2}{33s^4} - \frac{\sqrt{\frac{2}{7}}\beta^3t^2}{33s^4} - \frac{\sqrt{\frac{2}{7}}\beta^4\mu^5t}{11s^4} \\
 & + \frac{2\sqrt{\frac{2}{7}}\beta^4\mu^3t}{11s^4} - \frac{\sqrt{\frac{2}{7}}\beta^4\mu t}{11s^4} + \frac{\beta^3\mu^4}{11\sqrt{14}s^2} - \frac{\sqrt{\frac{2}{7}}\beta^3\mu^2}{11s^2} \\
 & + \frac{\beta^3}{11\sqrt{14}s^2} - \frac{5\beta^3\mu^5t}{33\sqrt{14}s^2} + \frac{5\sqrt{\frac{2}{7}}\beta^3\mu^3t}{33s^2} - \frac{5\beta^3\mu t}{33\sqrt{14}s^2}
 \end{aligned} \tag{B41}$$

$$\begin{aligned}
 [\bar{T}_{31}]_6^4 = & -\frac{\sqrt{\frac{2}{7}}\beta^4\mu^5t^5}{33s^4} + \frac{2\sqrt{\frac{2}{7}}\beta^4\mu^3t^5}{33s^4} - \frac{\sqrt{\frac{2}{7}}\beta^4\mu t^5}{33s^4} \\
 & - \frac{5\beta^3\mu^5t^5}{33\sqrt{14}s^4} + \frac{5\sqrt{\frac{2}{7}}\beta^3\mu^3t^5}{33s^4} - \frac{5\beta^3\mu t^5}{33\sqrt{14}s^4} \\
 & + \frac{\sqrt{\frac{2}{7}}\beta^4\mu^4t^4}{55s^4} - \frac{2\sqrt{\frac{2}{7}}\beta^4\mu^2t^4}{55s^4} + \frac{\sqrt{\frac{2}{7}}\beta^4t^4}{55s^4} \\
 & + \frac{\sqrt{\frac{2}{7}}\beta^3\mu^4t^4}{33s^4} - \frac{2\sqrt{\frac{2}{7}}\beta^3\mu^2t^4}{33s^4} + \frac{\sqrt{\frac{2}{7}}\beta^3t^4}{33s^4}
 \end{aligned} \tag{B42}$$

$$\begin{aligned}
 [\bar{T}_{12}]_6^5 = & \sqrt{1-\mu^2} \left\{ \frac{\beta^4\mu^4t}{60\sqrt{77}} - \frac{\beta^4\mu^2t}{30\sqrt{77}} + \frac{\beta^4t}{60\sqrt{77}} \right. \\
 & \left. + \frac{\beta^3\mu^4t}{12\sqrt{77}} - \frac{\beta^3\mu^2t}{6\sqrt{77}} + \frac{\beta^3t}{12\sqrt{77}} \right\}
 \end{aligned} \tag{B43}$$

$$\begin{aligned}
 [\bar{T}_{23}]_6^5 = & \sqrt{1-\mu^2} \left\{ \frac{\beta^3\mu^4t^3}{12\sqrt{77}s^4} - \frac{\beta^3\mu^2t^3}{6\sqrt{77}s^4} + \frac{\beta^3t^3}{12\sqrt{77}s^4} \right. \\
 & + \frac{\beta^4\mu^5t^2}{10\sqrt{77}s^4} - \frac{\beta^4\mu^3t^2}{5\sqrt{77}s^4} + \frac{\beta^4\mu t^2}{10\sqrt{77}s^4} \\
 & - \frac{\beta^4\mu^4t}{20\sqrt{77}s^4} + \frac{\beta^4\mu^2t}{10\sqrt{77}s^4} - \frac{\beta^4t}{20\sqrt{77}s^4} \\
 & \left. - \frac{\beta^3\mu^4t}{12\sqrt{77}s^2} + \frac{\beta^3\mu^2t}{6\sqrt{77}s^2} - \frac{\beta^3t}{12\sqrt{77}s^2} \right\}
 \end{aligned} \tag{B44}$$

$$\begin{aligned}
 [\bar{T}_{31}]_6^5 = & \sqrt{1-\mu^2} \left\{ -\frac{\beta^4\mu^4t^5}{60\sqrt{77}s^4} + \frac{\beta^4\mu^2t^5}{30\sqrt{77}s^4} - \frac{\beta^4t^5}{60\sqrt{77}s^4} \right. \\
 & \left. - \frac{\beta^3\mu^4t^5}{12\sqrt{77}s^4} + \frac{\beta^3\mu^2t^5}{6\sqrt{77}s^4} - \frac{\beta^3t^5}{12\sqrt{77}s^4} \right\}
 \end{aligned} \tag{B45}$$

$$[\bar{T}_{23}]_6^6 = -\frac{\beta^4\mu^6t^2}{60\sqrt{231}s^4} + \frac{\beta^4\mu^4t^2}{20\sqrt{231}s^4} - \frac{\beta^4\mu^2t^2}{20\sqrt{231}s^4} + \frac{\beta^4t^2}{60\sqrt{231}s^4} \tag{B46}$$

$$\begin{aligned}
 [\bar{T}_{12}]_8^0 = & -\frac{112\beta^4\mu^4}{1287} + \frac{32\beta^4\mu^2}{429} - \frac{16\beta^4}{2145} + \frac{56}{715}\beta^4\mu^5t \\
 & - \frac{112\beta^4\mu^3t}{1287} + \frac{32\beta^4\mu^3}{1287t} + \frac{8}{429}\beta^4\mu t - \frac{32\beta^4\mu}{2145t}
 \end{aligned} \tag{B47}$$

$$\begin{aligned}
 [\bar{T}_{23}]_8^0 = & \frac{56\beta^4\mu^4}{429s^4} - \frac{16\beta^4\mu^2}{143s^4} + \frac{8\beta^4}{715s^4} + \frac{28\beta^4\mu^6t^2}{195s^4} \\
 & - \frac{28\beta^4\mu^4t^2}{143s^4} + \frac{28\beta^4\mu^2t^2}{429s^4} - \frac{4\beta^4t^2}{1287s^4} - \frac{168\beta^4\mu^5t}{715s^4} \\
 & + \frac{112\beta^4\mu^3t}{429s^4} - \frac{32\beta^4\mu^3}{1287s^4t} - \frac{8\beta^4\mu t}{143s^4} + \frac{32\beta^4\mu}{2145s^4t}
 \end{aligned} \tag{B48}$$

$$\begin{aligned}
 [\bar{T}_{31}]_8^0 = & -\frac{56\beta^4\mu^5t^5}{715s^4} + \frac{112\beta^4\mu^3t^5}{1287s^4} - \frac{8\beta^4\mu t^5}{429s^4} \\
 & + \frac{56\beta^4\mu^4t^4}{429s^4} - \frac{16\beta^4\mu^2t^4}{143s^4} + \frac{8\beta^4t^4}{715s^4} - \frac{32\beta^4\mu^3t^3}{429s^4} \\
 & + \frac{32\beta^4\mu t^3}{715s^4} + \frac{32\beta^4\mu^2t^2}{2145s^4} - \frac{32\beta^4t^2}{6435s^4}
 \end{aligned} \tag{B49}$$

$$\begin{aligned}
 [\bar{T}_{12}]_8^1 = & \sqrt{1-\mu^2} \left\{ -\frac{112\sqrt{2}\beta^4\mu^3}{2145} + \frac{16}{715}\sqrt{2}\beta^4\mu \right. \\
 & + \frac{7}{143}\sqrt{2}\beta^4\mu^4t - \frac{14}{429}\sqrt{2}\beta^4\mu^2t \\
 & \left. + \frac{2\sqrt{2}\beta^4\mu^2}{143t} + \frac{1}{429}\sqrt{2}\beta^4t - \frac{2\sqrt{2}\beta^4}{715t} \right\}
 \end{aligned} \tag{B50}$$

$$\begin{aligned}
 [\bar{T}_{23}]_8^1 = & \sqrt{1-\mu^2} \left\{ \frac{56\sqrt{2}\beta^4\mu^3}{715s^4} - \frac{24\sqrt{2}\beta^4\mu}{715s^4} + \frac{6\sqrt{2}\beta^4\mu^5t^2}{65s^4} \right. \\
 & - \frac{12\sqrt{2}\beta^4\mu^3t^2}{143s^4} + \frac{2\sqrt{2}\beta^4\mu t^2}{143s^4} - \frac{21\sqrt{2}\beta^4\mu^4t}{143s^4} \\
 & \left. + \frac{14\sqrt{2}\beta^4\mu^2t}{143s^4} - \frac{2\sqrt{2}\beta^4\mu^2}{143s^4t} - \frac{\sqrt{2}\beta^4t}{143s^4} + \frac{2\sqrt{2}\beta^4}{715s^4t} \right\}
 \end{aligned} \tag{B51}$$

$$\begin{aligned}
 [\bar{T}_{31}]_8^1 = \sqrt{1-\mu^2} \left\{ -\frac{7\sqrt{2}\beta^4\mu^4t^5}{143s^4} + \frac{14\sqrt{2}\beta^4\mu^2t^5}{429s^4} \right. \\
 - \frac{\sqrt{2}\beta^4t^5}{429s^4} + \frac{56\sqrt{2}\beta^4\mu^3t^4}{715s^4} - \frac{24\sqrt{2}\beta^4\mu t^4}{715s^4} \\
 \left. - \frac{6\sqrt{2}\beta^4\mu^2t^3}{143s^4} + \frac{6\sqrt{2}\beta^4t^3}{715s^4} + \frac{16\sqrt{2}\beta^4\mu t^2}{2145s^4} \right\} \quad (B52)
 \end{aligned}$$

$$\begin{aligned}
 [\bar{T}_{12}]_8^2 = \frac{16}{429}\sqrt{\frac{7}{5}}\beta^4\mu^4 - \frac{128\beta^4\mu^2}{429\sqrt{35}} + \frac{16\beta^4}{429\sqrt{35}} \\
 - \frac{8}{143}\sqrt{\frac{5}{7}}\beta^4\mu^5t + \frac{32}{429}\sqrt{\frac{5}{7}}\beta^4\mu^3t \\
 - \frac{8\beta^4\mu^3}{143\sqrt{35}t} - \frac{8}{429}\sqrt{\frac{5}{7}}\beta^4\mu t + \frac{8\beta^4\mu}{143\sqrt{35}t} \quad (B53)
 \end{aligned}$$

$$\begin{aligned}
 [\bar{T}_{23}]_8^2 = -\frac{8\sqrt{\frac{7}{5}}\beta^4\mu^4}{143s^4} + \frac{64\beta^4\mu^2}{143\sqrt{35}s^4} - \frac{8\beta^4}{143\sqrt{35}s^4} \\
 - \frac{3\sqrt{\frac{5}{7}}\beta^4\mu^6t^2}{26s^4} + \frac{51\sqrt{\frac{5}{7}}\beta^4\mu^4t^2}{286s^4} - \frac{19\sqrt{\frac{5}{7}}\beta^4\mu^2t^2}{286s^4} \\
 + \frac{\sqrt{\frac{5}{7}}\beta^4t^2}{286s^4} + \frac{24\sqrt{\frac{5}{7}}\beta^4\mu^5t}{143s^4} - \frac{32\sqrt{\frac{5}{7}}\beta^4\mu^3t}{143s^4} \\
 + \frac{8\beta^4\mu^3}{143\sqrt{35}s^4t} + \frac{8\sqrt{\frac{5}{7}}\beta^4\mu t}{143s^4} - \frac{8\beta^4\mu}{143\sqrt{35}s^4t} \quad (B54)
 \end{aligned}$$

$$\begin{aligned}
 [\bar{T}_{31}]_8^2 = \frac{8\sqrt{\frac{5}{7}}\beta^4\mu^5t^5}{143s^4} - \frac{32\sqrt{\frac{5}{7}}\beta^4\mu^3t^5}{429s^4} + \frac{8\sqrt{\frac{5}{7}}\beta^4\mu t^5}{429s^4} \\
 - \frac{8\sqrt{\frac{7}{5}}\beta^4\mu^4t^4}{143s^4} + \frac{64\beta^4\mu^2t^4}{143\sqrt{35}s^4} - \frac{8\beta^4t^4}{143\sqrt{35}s^4} \\
 + \frac{24\beta^4\mu^3t^3}{143\sqrt{35}s^4} - \frac{24\beta^4\mu t^3}{143\sqrt{35}s^4} - \frac{8\beta^4\mu^2t^2}{429\sqrt{35}s^4} + \frac{8\beta^4t^2}{429\sqrt{35}s^4} \quad (B55)
 \end{aligned}$$

$$\begin{aligned}
 [\bar{T}_{12}]_8^3 = \sqrt{1-\mu^2} \left\{ \frac{16}{39}\sqrt{\frac{2}{1155}}\beta^4\mu^3 - \frac{16}{39}\sqrt{\frac{2}{1155}}\beta^4\mu \right. \\
 - \frac{1}{13}\sqrt{\frac{15}{154}}\beta^4\mu^4t + \frac{5}{39}\sqrt{\frac{10}{231}}\beta^4\mu^2t \\
 \left. - \frac{2\sqrt{\frac{2}{1155}}\beta^4\mu^2}{39t} - \frac{1}{39}\sqrt{\frac{5}{462}}\beta^4t + \frac{2\sqrt{\frac{2}{1155}}\beta^4}{39t} \right\} \quad (B56)
 \end{aligned}$$

$$\begin{aligned}
 [\bar{T}_{23}]_8^3 = \sqrt{1-\mu^2} \left\{ -\frac{8\sqrt{\frac{2}{1155}}\beta^4\mu^3}{13s^4} + \frac{8\sqrt{\frac{2}{1155}}\beta^4\mu}{13s^4} \right. \\
 - \frac{\sqrt{\frac{110}{21}}\beta^4\mu^5t^2}{39s^4} + \frac{2\sqrt{\frac{70}{33}}\beta^4\mu^3t^2}{39s^4} \\
 - \frac{\sqrt{\frac{10}{231}}\beta^4\mu t^2}{13s^4} + \frac{3\sqrt{\frac{15}{154}}\beta^4\mu^4t}{13s^4} - \frac{5\sqrt{\frac{10}{231}}\beta^4\mu^2t}{13s^4} \\
 \left. + \frac{2\sqrt{\frac{2}{1155}}\beta^4\mu^2}{39s^4t} + \frac{\sqrt{\frac{5}{462}}\beta^4t}{13s^4} - \frac{2\sqrt{\frac{2}{1155}}\beta^4}{39s^4t} \right\} \quad (B57)
 \end{aligned}$$

$$\begin{aligned}
 [\bar{T}_{31}]_8^3 = \sqrt{1-\mu^2} \left\{ \frac{\sqrt{\frac{15}{154}}\beta^4\mu^4t^5}{13s^4} - \frac{5\sqrt{\frac{10}{231}}\beta^4\mu^2t^5}{39s^4} \right. \\
 + \frac{\sqrt{\frac{5}{462}}\beta^4t^5}{39s^4} - \frac{8\sqrt{\frac{2}{1155}}\beta^4\mu^3t^4}{13s^4} + \frac{8\sqrt{\frac{2}{1155}}\beta^4\mu t^4}{13s^4} \\
 \left. + \frac{2\sqrt{\frac{2}{1155}}\beta^4\mu^2t^3}{13s^4} - \frac{2\sqrt{\frac{2}{1155}}\beta^4t^3}{13s^4} \right\} \quad (B58)
 \end{aligned}$$

$$\begin{aligned}
 [\bar{T}_{12}]_8^4 = -\frac{4}{195}\sqrt{\frac{2}{77}}\beta^4\mu^4 + \frac{8}{195}\sqrt{\frac{2}{77}}\beta^4\mu^2 - \frac{4}{195}\sqrt{\frac{2}{77}}\beta^4 \\
 + \frac{2}{39}\sqrt{\frac{2}{77}}\beta^4\mu^5t - \frac{4}{39}\sqrt{\frac{2}{77}}\beta^4\mu^3t + \frac{2}{39}\sqrt{\frac{2}{77}}\beta^4\mu t \quad (B59)
 \end{aligned}$$

$$\begin{aligned}
 [\bar{T}_{23}]_8^4 = \frac{2\sqrt{\frac{2}{77}}\beta^4\mu^4}{65s^4} - \frac{4\sqrt{\frac{2}{77}}\beta^4\mu^2}{65s^4} + \frac{2\sqrt{\frac{2}{77}}\beta^4}{65s^4} + \frac{\sqrt{\frac{22}{7}}\beta^4\mu^6t^2}{65s^4} \\
 - \frac{23\sqrt{\frac{2}{77}}\beta^4\mu^4t^2}{65s^4} + \frac{\sqrt{\frac{2}{77}}\beta^4\mu^2t^2}{5s^4} - \frac{\sqrt{\frac{2}{77}}\beta^4t^2}{65s^4} \\
 - \frac{2\sqrt{\frac{2}{77}}\beta^4\mu^5t}{13s^4} + \frac{4\sqrt{\frac{2}{77}}\beta^4\mu^3t}{13s^4} - \frac{2\sqrt{\frac{2}{77}}\beta^4\mu t}{13s^4} \quad (B60)
 \end{aligned}$$

$$\begin{aligned}
 [\bar{T}_{31}]_8^4 = -\frac{2\sqrt{\frac{2}{77}}\beta^4\mu^5t^5}{39s^4} + \frac{4\sqrt{\frac{2}{77}}\beta^4\mu^3t^5}{39s^4} - \frac{2\sqrt{\frac{2}{77}}\beta^4\mu t^5}{39s^4} \\
 + \frac{2\sqrt{\frac{2}{77}}\beta^4\mu^4t^4}{65s^4} - \frac{4\sqrt{\frac{2}{77}}\beta^4\mu^2t^4}{65s^4} + \frac{2\sqrt{\frac{2}{77}}\beta^4t^4}{65s^4} \quad (B61)
 \end{aligned}$$

$$[\bar{T}_{12}]_8^5 = \sqrt{1-\mu^2} \left\{ \frac{\beta^4\mu^4t}{15\sqrt{2002}} - \frac{1}{15}\sqrt{\frac{2}{1001}}\beta^4\mu^2t + \frac{\beta^4t}{15\sqrt{2002}} \right\} \quad (B62)$$

$$\begin{aligned}
 [\bar{T}_{23}]_8^5 = \sqrt{1-\mu^2} \left\{ \frac{\sqrt{\frac{2}{1001}}\beta^4\mu^5t^2}{5s^4} - \frac{2\sqrt{\frac{2}{1001}}\beta^4\mu^3t^2}{5s^4} \right. \\
 + \frac{\sqrt{\frac{2}{1001}}\beta^4\mu t^2}{5s^4} - \frac{\beta^4\mu^4t}{5\sqrt{2002}s^4} \\
 \left. + \frac{\sqrt{\frac{2}{1001}}\beta^4\mu^2t}{5s^4} - \frac{\beta^4t}{5\sqrt{2002}s^4} \right\} \quad (B63)
 \end{aligned}$$

$$\begin{aligned}
 [\bar{T}_{31}]_8^5 = \sqrt{1-\mu^2} \left\{ -\frac{\beta^4\mu^4t^5}{15\sqrt{2002}s^4} \right. \\
 \left. + \frac{\sqrt{\frac{2}{1001}}\beta^4\mu^2t^5}{15s^4} - \frac{\beta^4t^5}{15\sqrt{2002}s^4} \right\} \quad (B64)
 \end{aligned}$$

$$[\bar{T}_{23}]_8^6 = -\frac{\beta^4\mu^6t^2}{30\sqrt{429}s^4} + \frac{\beta^4\mu^4t^2}{10\sqrt{429}s^4} - \frac{\beta^4\mu^2t^2}{10\sqrt{429}s^4} + \frac{\beta^4t^2}{30\sqrt{429}s^4} \quad (B65)$$

$[\bar{T}_{12}]_6^6, [\bar{T}_{31}]_6^6, [\bar{T}_{12}]_8^6, [\bar{T}_{31}]_8^6$  and all the moments of  $T$ -terms for  $\ell = 8$  and  $m = 7, 8$  are zero.